

# TRAF1 is a key mediator for hepatic ischemia/reperfusion injury

X-F Zhang<sup>1,5</sup>, R Zhang<sup>2,5</sup>, L Huang<sup>3,4,5</sup>, P-X Wang<sup>3,4</sup>, Y Zhang<sup>3,4</sup>, D-S Jiang<sup>3,4</sup>, L-H Zhu<sup>3,4</sup>, S Tian<sup>3,4</sup>, X-D Zhang<sup>\*1</sup> and H Li<sup>\*3,4</sup>

Tumor necrosis factor receptor-associated factor 1 (TRAF1), an adapter in signal transduction, is involved in immunity and in apoptotic processes in various cell types. However, little is known about its function and the molecular mechanism of its activation during liver injury. This study tested the hypothesis that TRAF1 is a mediator of cell injury after hepatic ischemia/reperfusion injury (I/R). In a mouse hepatic I/R injury model, we found that TRAF1 expression was highly induced. TRAF1 deficiency was liver protective, whereas sustained TRAF1 overexpression aggravated liver injury in response to hepatic I/R injury. Mechanistic studies demonstrated that a deficiency of TRAF1 in cultured hepatocytes led to the inhibition of NF- $\kappa$ B-mediated inflammatory responses, suppression of the ASK/JNK pro-death pathway and promotion of cellular regeneration capacity. In contrast, the converse occurred in hepatocyte-specific TRAF1 transgenic mice. TRAF1 activated the ASK1/JNK pathway and promoted hepatic injury. Our study demonstrates that TRAF1 is a crucial early mediator of hepatic I/R injury and suggests that TRAF1 may be a potential gene therapy target for the treatment of liver injury.

*Cell Death and Disease* (2014) 5, e1467; doi:10.1038/cddis.2014.411; published online 16 October 2014

Ischemia-reperfusion injury (I/R) is responsible for primary liver dysfunction and failure after transplantation, liver resection, or hemorrhagic shock.<sup>1</sup> I/R injury is triggered when the liver is transiently deprived of oxygen and reoxygenated, and this type of injury can occur in several clinical settings, such as those associated with low-flow states, a diverse range of surgical procedures, or organ procurement for transplantation.<sup>2</sup> Jaeschke *et al.*<sup>3</sup> described and characterized two distinct phases of liver injury. The early phase of injury occurs during the initial few hours after reperfusion and involves the production of reactive oxygen species by Kupffer cells, which also produce pro-inflammatory cytokines, including tumor necrosis factor- $\alpha$  (TNF- $\alpha$ ) and interleukin-1 (IL-1), and eventually give rise to a later, inflammation-mediated, phase of injury.<sup>3</sup> I/R injury is detrimental to liver graft function. Unfortunately, there is no treatment available to prevent hepatic I/R injury. A better understanding of the intrinsic mechanisms that mediate the intricate cell survival signaling pathway should allow the development of a novel therapeutic approach to minimize the adverse effects of I/R injury.

Nuclear factor-kappa B (NF- $\kappa$ B) and activating protein-1 (AP-1) are important transcription factors that control the

expression of cytokines and factors involved in the regulation of I/R injury. Previous studies have indicated that NF- $\kappa$ B is activated during liver I/R injury and that the inhibition of its activation during I/R reduces hepatocyte necrosis in rats.<sup>4–7</sup> The inflammatory response is tightly regulated by pro-inflammatory mediators such as p38 mitogen-activated protein kinases (MAPKs) and c-Jun-N-terminal kinase (JNK). The activation of JNK is crucial to I/R injury and leads to caspase-3 activation and hepatic apoptosis.<sup>8</sup> Under I/R conditions, JNK is activated by phosphorylation, translocates to the nucleus, and activates target genes such as c-Jun. Phosphorylated c-Jun can dimerize, leading to the formation of AP-1, which is involved in the transcription of a wide variety of proteins, including some proapoptotic proteins. NF- $\kappa$ B/JNK pathways are crucial for the pathogenesis of liver I/R injury, but how these pathways are regulated in I/R injury is largely unknown.

The tumor necrosis factor receptor (TNF-R)-associated factor (TRAF) family of intracellular proteins includes seven known members (TRAF1–7) in mammals, and these proteins have been characterized as signaling adapters that bind directly to TNF-R superfamily receptors. TRAF1 is unique

<sup>1</sup>College of Life Sciences, Wuhan University, Wuhan, PR China; <sup>2</sup>National Laboratory of Medical Molecular Biology, Institute of Basic Medical Sciences, Chinese Academy of Medical Sciences and Peking Union Medical College, Beijing, China; <sup>3</sup>Department of Cardiology, Renmin Hospital of Wuhan University, Wuhan, China and <sup>4</sup>Cardiovascular Research Institute, Wuhan University, Wuhan, China

\*Corresponding author: H Li, Department of Cardiology, Renmin Hospital of Wuhan University, Cardiovascular Research Institute, Wuhan University, Jiefang Road 238, Wuhan 430060, PR China. Tel/Fax: +86 27 88076990; E-mail: lihl@whu.edu.cn

or X-D Zhang, College of Life Sciences, Wuhan University, LuoJiaShan, Wuchang, Wuhan 430072, PR China. Tel/Fax: +86 27 68756606; E-mail: zhangxd@whu.edu.cn

<sup>5</sup>These authors contributed equally to this work.

**Abbreviations:** Ad, adeno-virus; ALT, alanine aminotransferase; ASK1, apoptosis signal-regulating kinase 1; AST, aspartate aminotransferase; Bax, B-cell lymphoma 2-associated X protein; Bcl-2, B-cell lymphoma 2; Bcl-XL, Bcl-extra large; Bad, Bcl-2-associated death promoter; Bid, BH3-interacting-domain death agonist; Bak, Bcl-2 antagonist killer; Cyt C, cytochrome C; COX II, cytochrome c oxidase subunit II; DAPI, 4',6-diamidino-2-phenylindole; Dn, dominant-negative; FRET, fluorescence resonance energy transfer; H/R, hypoxia/reoxygenation; IgG, immunoglobulin G; IL, interleukin; IP, immunoprecipitation; I/R, ischemia/reperfusion; Ly6G, lymphocyte antigen 6 complex locus G; JNK, c-Jun-N-terminal kinase; KO, knockout; LDH, lactate dehydrogenase; MAC1, macrophage antigen-1; MAPK, mitogen-activated protein kinase; MKK, mitogen-activated protein kinase kinase; MPO, myeloperoxidase; mRNA, messenger RNA; MTT, 3-(4,5-Dimethylthiazol-2-yl)-2, 5-diphenyltetrazolium bromide; NF- $\kappa$ B, Nuclear Factor-kappa B; NTG, non-transgenic; PCNA, proliferating cell nuclear antigen; shRNA, short hairpin RNA; TG, transgenic; TNF- $\alpha$ , tumor necrosis factor- $\alpha$ ; TRAF1, tumor necrosis factor receptor-associated factor 1; TUNEL, terminal deoxynucleotidyl transferase-mediated deoxyuridine triphosphate nick-end labeling; WT, wild type

Received 16.7.14; accepted 21.7.14; Edited by G Melino

among TRAFs in that it lacks the RING domain,<sup>9,10</sup> and its expression is restricted to activated lymphocytes, dendritic cells, and certain epithelia.<sup>11</sup> TRAF1 can be significantly induced by stimulation of TNF- $\alpha$  or other ligands<sup>12</sup> and is dysregulated in diseases involving atheromas,<sup>13</sup> lymphomas,<sup>11</sup> and solid tumors.<sup>14</sup> TRAF1 exerts diverse and often conflicting biologic effects that are cell-type- and context-specific.<sup>15,16</sup> Numerous studies have provided evidence that TRAF1 participates in the NF- $\kappa$ B pathway and has an antiapoptotic role in TNF- $\alpha$ -mediated hepatocyte apoptosis.<sup>17,18</sup> However, Tsitsikov *et al.*<sup>19</sup> reported marked proliferation of TRAF1-deficient T cells in response to TNF- $\alpha$  treatment and noted that TRAF1-null mice were hypersensitive to TNF-induced skin necrosis. TRAF1 can be cleaved by caspase-8, resulting in the negative regulation of the antiapoptotic role of TRAF2 during TNF-induced apoptosis.<sup>20</sup> In addition, our previous work suggests that TRAF1 acts as a proapoptotic mediator in MCAO-induced ischaemic stroke.<sup>21</sup> As liver I/R results in inflammation and the death of hepatocytes, we hypothesized that TRAF1 contributes to the pathogenesis of liver I/R.

This study tested the hypothesis that TRAF1 is a critical mediator of cell injury after hepatic I/R. We demonstrated that TRAF1 expression was induced in mouse hepatocytes 3 h after I/R injury. Moreover, we found that the disruption of TRAF1 was liver-protective, whereas sustained TRAF1 overexpression was associated with increased inflammatory responses, susceptibility to ischemia-induced apoptosis, and

a decreased liver regenerative capacity. We further revealed that the inhibition of the JNK pro-death pathway and NF- $\kappa$ B pathway is crucial for the increased survival of hepatocytes mediated by TRAF1 inhibition, implicating a TRAF1-ASK1 interaction in hepatic I/R.

## Results

**Hepatic TRAF1 messenger RNA and protein expression were induced in liver I/R injury.** We first determined whether TRAF1 is involved in liver I/R injury by analyzing its expression in ischemic lobes from mice subjected to warm liver I/R and from mice subjected to a sham procedure. TRAF1 messenger RNA (mRNA) levels gradually increased after reperfusion and reached peak levels at 48 h (Figure 1a). A western blot analysis revealed that TRAF1 protein expression was significantly upregulated after ischemia and persisted after 24 h of reperfusion, but had slightly decreased after 48 h (Figure 1b). In cultured hepatocytes exposed to hypoxia/reoxygenation (H/R) injury, we also detected a similar upregulation of the TRAF1 protein over time (Figure 1c). These results support a possible role for TRAF1 in mediating liver I/R injury.

**TRAF1 is involved in liver I/R injury.** As TRAF1 was highly upregulated on exposure to I/R, we next characterized the effect of TRAF1 suppression on I/R-induced injury. Western

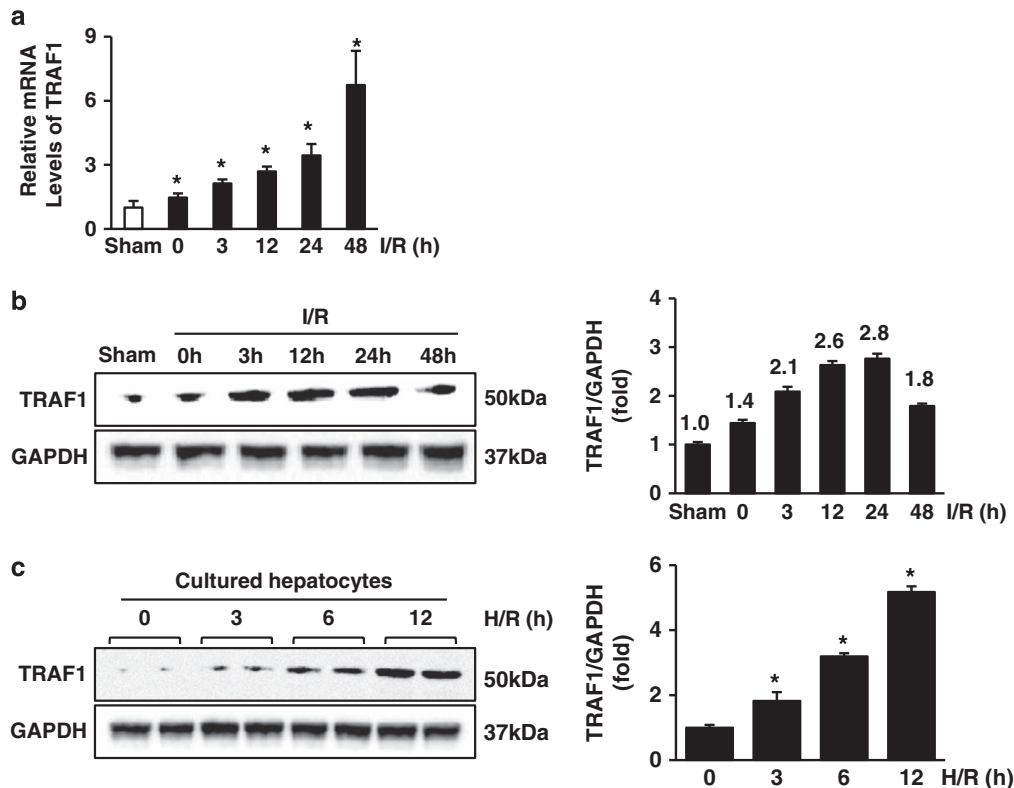


**Figure 1** Hepatic TRAF1 is upregulated after liver I/R injury. (a) Relative TRAF1 expression in hepatic tissues quantified by qRT-PCR at the indicated time points following ischemic onset ( $n=9$  per time point,  $*P<0.05$  versus sham). (b) Western blot analysis for TRAF1 detection in protein extracts from hepatic tissues at the indicated time points following ischemic onset (left). Values were normalized to GAPDH. Right panel: quantification of TRAF1 levels (right,  $n=3$  per time point; the number on the bar represents the fold change). (c) Western blot analysis of TRAF1 expression in cultured hepatocytes after H/R injury (left) and the quantification of TRAF1 levels (right,  $n=6$  per time point, right,  $*P<0.05$  versus sham). Data are presented as the mean  $\pm$  S.D.

blot analysis of liver tissues from global TRAF1-knockout (KO) and wild-type (WT) mice indicated that TRAF1 was absent in the TRAF1-KO mice (Figure 2a). The mice were subjected to hepatic I/R, and liver architecture and morphology were assessed by histopathology 12, 24, and 48 h after reperfusion. No significant differences were observed between the KO and WT group after the sham operation. Extensive necrosis was present in the WT group, whereas TRAF1 deficiency resulted in substantially smaller necrotic areas (Figure 2b). After warm partial hepatic I/R, the levels of the serum markers ALT and AST in the WT and TRAF1-KO mice were higher than that in the sham group. Significantly lower ALT and AST levels were noted in TRAF1-deficient mice than that in WT mice (Figure 2c), which further indicated that these mice experience less liver damage following I/R injury.

TRAF1 is expressed in both hepatocytes and cells of the myeloid-lineage and may function in a cell-type-specific manner. To determine the origin of TRAF1 that contributes to I/R injury, we established transgenic (TG) mice expressing TRAF1 under the control of either a myeloid-specific lysozyme M promoter or the hepatocyte-specific albumin (Alb) promoter and enhancer (Figure 2d). Compared with non-transgenic (NTG) mice, the serum ALT/AST levels in Alb-TRAF1 TG mice were higher 24 h after I/R, with significant hepatic necrosis observed in H&E-stained liver sections, whereas the injury in the Lys-M-TRAF1 TG mice remained comparable to that in the NTG control (Figures 2e, f). These results indicate that hepatocytes have a major role in TRAF1-mediated injury, and we focused further research on only the hepatocyte-specific TRAF1 TG mice (Figure 2g). The livers in TRAF1 TG mice exhibited significant histological injury and higher serum ALT/AST levels 12, 24, and 48 h after I/R than NTG controls (Figures 2h, i).

**TRAF1 contributes to the inflammatory response after liver I/R.** Previous investigations have revealed that polymorphonuclear cells (PMNs) and other immune cells begin to accumulate during the initial reperfusion period.<sup>22</sup> Myeloperoxidase (MPO) activity, which is an activation index of PMNs, was lower in TRAF1-KO mice than in WT mice but higher in TRAF1 TG mice than in NTG mice after liver I/R (Figure 3a). The accumulation of T cells, neutrophils, and macrophages in the post-ischemic liver lobes was assessed by immunofluorescent staining with antibodies specific for cells' surface markers: CD3, lymphocyte antigen 6 complex locus G (LY6G), and macrophage antigen-1 (MAC1), respectively. The number of positive cells was significantly lower in livers from TRAF1-deficient mice, whereas the number was higher in TRAF1 TG mice (Figures 3b and c). The cells labeled with surface markers were also assessed by flow cytometry, and results similar to those found above were observed (Figure 3d), indicating that TRAF1 is essential for the I/R-induced migration of inflammatory cells.

The local mRNA expression of the pro-inflammatory factors TNF- $\alpha$ , IFN $\gamma$ , IL-1 $\beta$ , IL-2, and IL-6 and the anti-inflammatory factor IL-10 was examined after 60 min of ischemia and 12 h of reperfusion in each group. Partial hepatic I/R in the WT mice induced a marked upregulation of pro-inflammatory cytokine levels and decreased IL-10 expression compared with the

sham-operated controls. However, TRAF1 deficiency significantly reduced the cytokine expression (Figure 3e). The TNF- $\alpha$ , IL-1 $\beta$ , IL-2, and IL-6 levels in the peripheral blood were consistently significantly lower, and the IL-10 levels were higher in TRAF1-deficient mice than in WT mice after reperfusion (Figure 3g). In contrast, local and circulating pro-inflammatory cytokine levels were higher, and the IL-10 levels were lower in the TRAF1-overexpressing mice than in the NTG group (Figures 3f, h).

TRAF1 has been suggested to regulate NF- $\kappa$ B activation.<sup>15</sup> In hepatocytes, NF- $\kappa$ B activation following I/R is responsible for the injury.<sup>22</sup> Thus, we measured the levels of the p65 subunit of NF- $\kappa$ B and the inhibitory protein I $\kappa$ B $\alpha$  and found increases in the p65 and I $\kappa$ B $\alpha$  phosphorylation levels after liver I/R. In the absence of TRAF1, liver I/R injury could no longer induce the phosphorylation of p65 and I $\kappa$ B $\alpha$  (Figure 3i), whereas TRAF1 overexpression exacerbated the NF- $\kappa$ B activation (Figure 3j). These results indicate that the lack of TRAF1 blunted the inflammatory insult induced by I/R.

#### TRAF1 has an important role in I/R-induced cell death.

The cellular apoptosis or necrosis level determines the extent of liver damage after I/R. To analyze the effects of TRAF1 on hepatocyte apoptosis, we first used a terminal deoxynucleotidyl transferase-mediated deoxyuridine triphosphate nick-end labeling (TUNEL) assay. The number of positively stained cells was diminished by the deletion of TRAF1 but was augmented in TRAF1-overexpressing mice (Figures 4a and b).

The activation of caspase-3 and B-cell lymphoma 2-associated X protein (Bax) and the decreased production of B-cell lymphoma 2 (Bcl-2) are major biochemical markers of apoptotic cell death, and various studies have described these events after liver I/R.<sup>23</sup> Thus, we examined the protein expression of these apoptotic markers in ischemic liver lobes and observed a significant decrease in the proapoptotic factors caspase-3, Bax, Bcl-2-associated death promoter (Bad), Bcl-2 antagonist killer (Bak) and BH3-interacting-domain death agonist (Bid) and an increase in the anti-apoptotic factors Bcl-2 and Bcl-extra large (Bcl-XL) in TRAF1-deficient mice (Figures 4c and e), whereas overexpressing TRAF1 induced higher levels of proapoptotic markers and lower levels of anti-apoptotic markers (Figures 4d and g). Cytochrome C (Cyt C) released from mitochondria into the cytoplasm activates downstream caspases and apoptosis. We observed a significant release of Cyt C in TRAF1 TG mice at 12 h after I/R, whereas TRAF1 deficiency prevented Cyt C release (Figures 4f, h).

#### TRAF1 regulates cultured hepatocyte survival after H/R.

To investigate whether TRAF1 is a modulator of hepatocyte cell death or survival during the I/R injury process, we constructed an *in vitro* system that mimics I/R stress on hepatocytes by subjecting hepatocytes to 60 min of hypoxia followed by a timed series of reoxygenation steps. The cultured hepatocytes isolated from TRAF1-deficient mice exhibited less DNA fragmentation and LDH release and higher values in the 3-(4,5-Dimethylthiazol-2-yl)-2, 5-diphenyltetrazolium bromide (MTT) assay results after H/R, demonstrating the protective effects of TRAF1 deficiency (Figure 5b). Notably, the survival

index after reoxygenation was significantly deteriorated in hepatocytes from TRAF1 TG mice than that from the NTG controls (Figure 5b).

We then used recombinant adenoviruses to evaluate the effect of TRAF1 on cultured hepatocytes. The transfection of cultured hepatocytes with AdshTRAF1 successfully silenced endogenous TRAF1 expression, and AdTRAF1 resulted in a significant increase in exogenous TRAF1 expression (Figure 5a). The primary hepatocytes transfected with AdshTRAF1 were significantly protected from H/R-mediated cell damage, and AdTRAF1 substantially impaired cell survival (Figure 5c). We further examined apoptotic markers to confirm the *in vitro* effects of hepatocyte TRAF1 on apoptosis induced by H/R. H/R challenges induced the expression of Bax and cleaved caspase-3, whereas suppressed the expression of Bcl-2; however, the effect was diminished in cells transfected with AdshTRAF1 and was greatly increased by transfection with AdTRAF1 (Figure 5d, e).

**The regenerative capacity of the liver was regulated by TRAF1.** Hepatocyte proliferation or regeneration can ameliorate hepatocyte injury after liver I/R, and the capacity of the liver to regenerate is an important determinant of post-ischemic liver function.<sup>24</sup> Therefore, we next investigated the effects of TRAF1 on hepatocyte proliferation, as assessed by

proliferating cell nuclear antigen (PCNA) staining. The TRAF1-KO mice exhibited a higher percentage of PCNA-positive cells than WT controls 24 h after liver I/R (Figure 6a), suggesting that enhanced hepatic regeneration occurs in TRAF1-deficient mice. The extent of hepatocellular regeneration following I/R was further assessed by measuring the mRNA and protein expression levels of the proliferation markers PCNA, cyclin D and cyclin E; the corresponding genes were induced in ischemic liver lobes from WT mice after I/R and were expressed at significantly higher levels in TRAF1-KO mice (Figures 6c and e). However, the number of PCNA-positive cells was lower in TRAF1-overexpressing livers, indicating diminished hepatocyte proliferation (Figure 6b). This finding was also confirmed by quantitative change in proliferation marker expression as examined by real-time PCR and western blotting (Figures 6d and f).

**TRAF1 promotes the ASK1-MKK4/7-JNK signaling pathway.** A three-tiered signaling module consisting of MAPKKKs (MKKKs), MAPKKs (MKKs), and MAPKs enables cells to respond to exogenous and endogenous stimuli.<sup>25</sup> Apoptosis signal-regulating kinase 1 (ASK1) is a member of the MAPKKK family and has been reported to be strongly activated by ischemia in the perfused rat heart.<sup>26</sup> Therefore, we initially assessed the phosphorylation level of ASK1, by

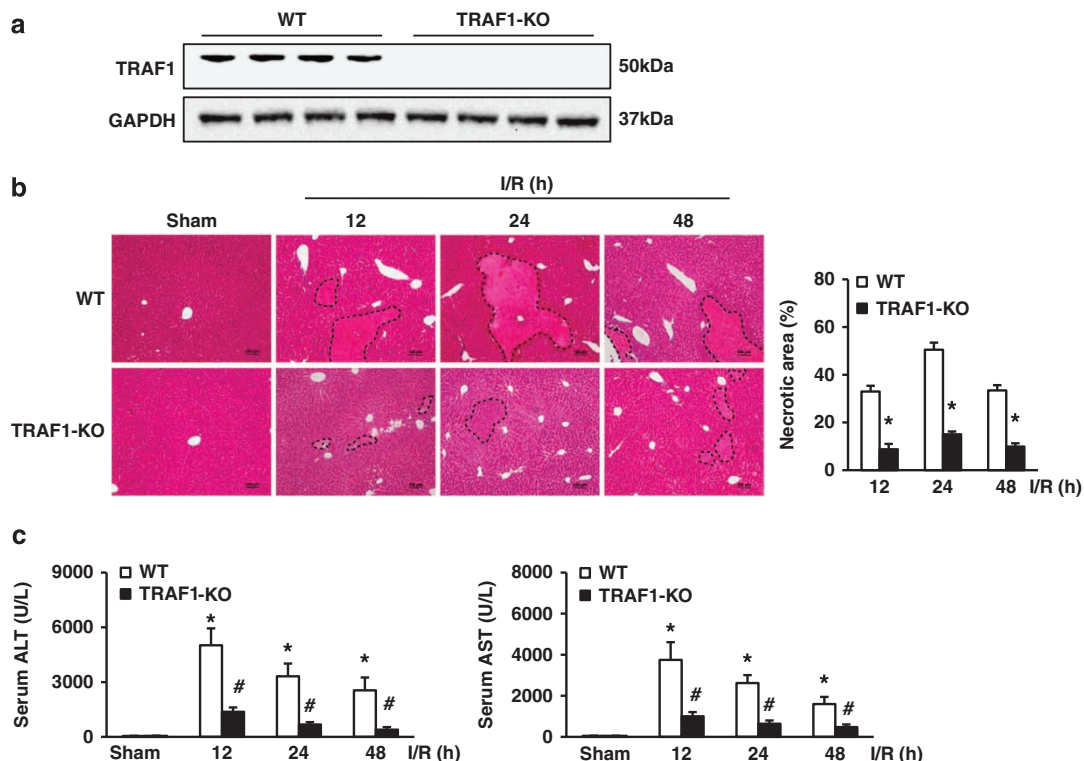


**Figure 2** TRAF1 participates in the regulation of liver I/R injury. (a) Western blot analysis of TRAF1 expression in liver tissues from TRAF1-KO and WT mice. (b, h) Representative images of the areas of focal necrosis in hepatic cells of the indicated mice at different time points after I/R (left). Scale bar: 100  $\mu$ m. Quantification of the necrotic areas (right;  $n = 8$  at each time point,  $*P < 0.05$  versus WT or NTG). (c, i) Quantification of serum marker ALT and AST levels at the indicated time points after I/R ( $n = 8$  at each time point,  $*P < 0.05$  versus sham,  $\#P < 0.05$  versus I/R). (d) Schematic representation of two transgene constructs. (e) Representative images of liver I/R injury and quantification of necrotic areas ( $n = 8$ ,  $\#P < 0.05$  versus NTG). (f) Quantification of serum ALT and AST levels. (g) Western blot analysis of TRAF1 detection in hepatic tissues from four founder lines of TRAF1 TG mice (TG1–TG4) and NTG mice and relative TRAF1 levels in TG1–TG4 and NTG mice (the number on the bar represents the fold-change). Data are presented as the mean  $\pm$  S.D.



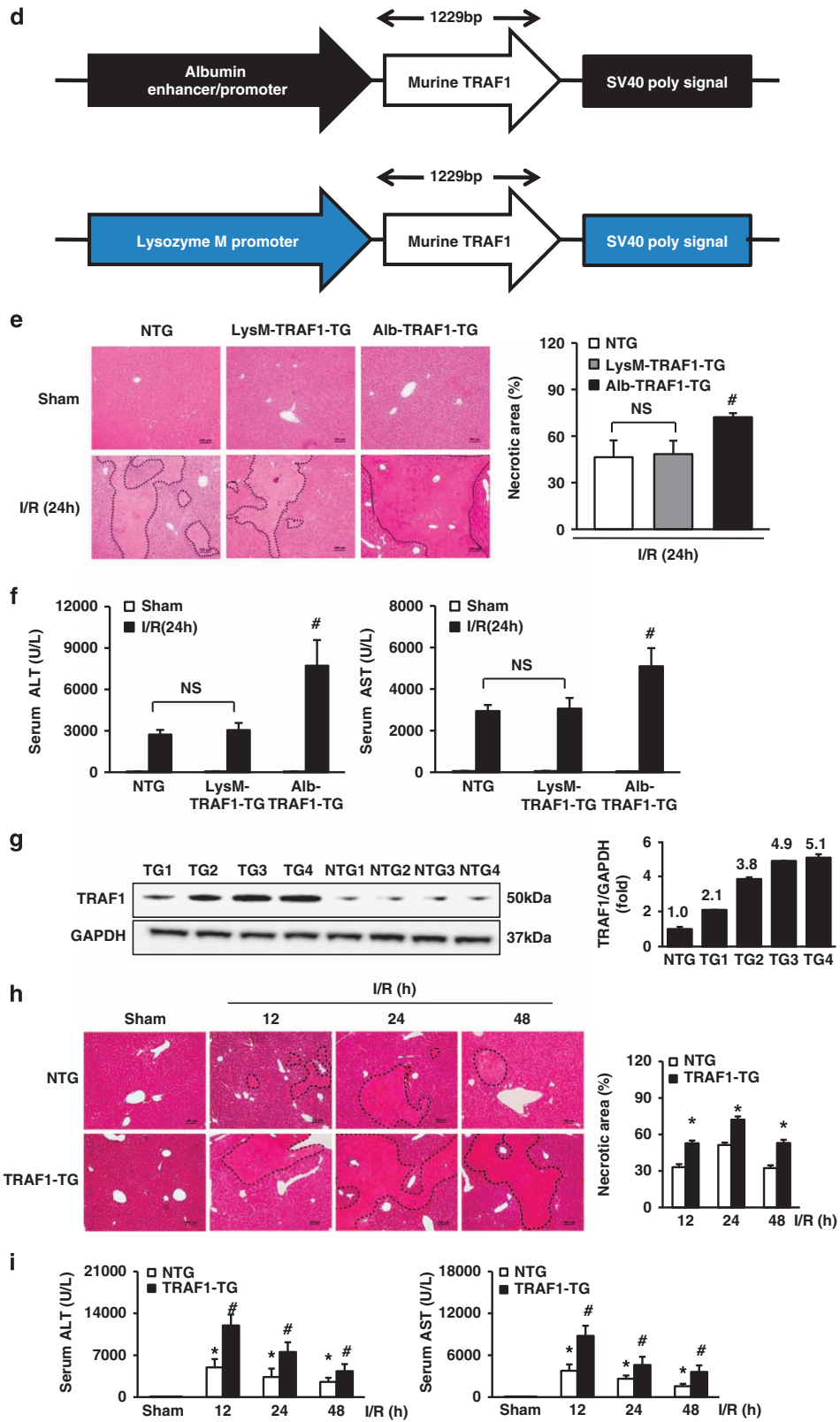
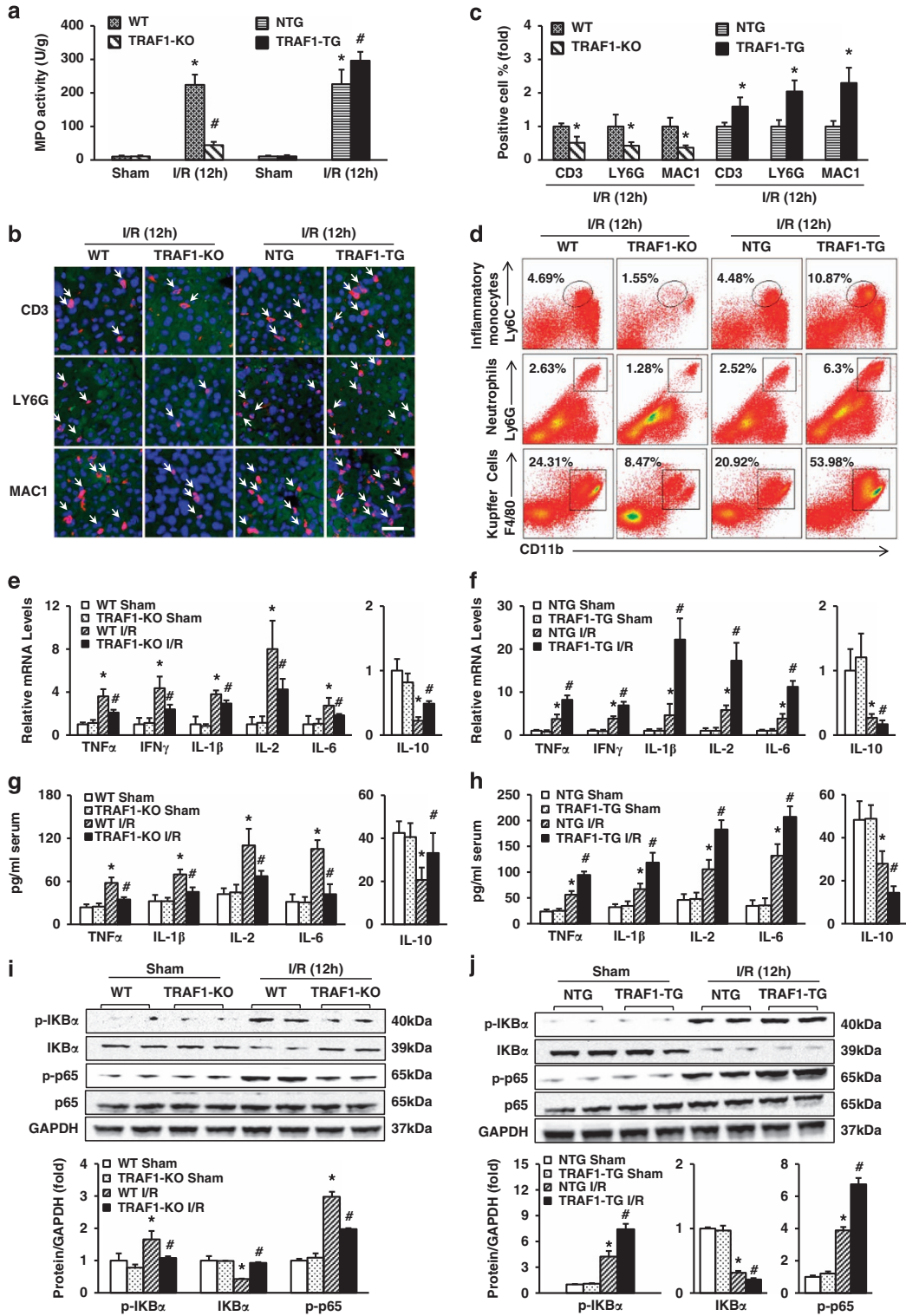
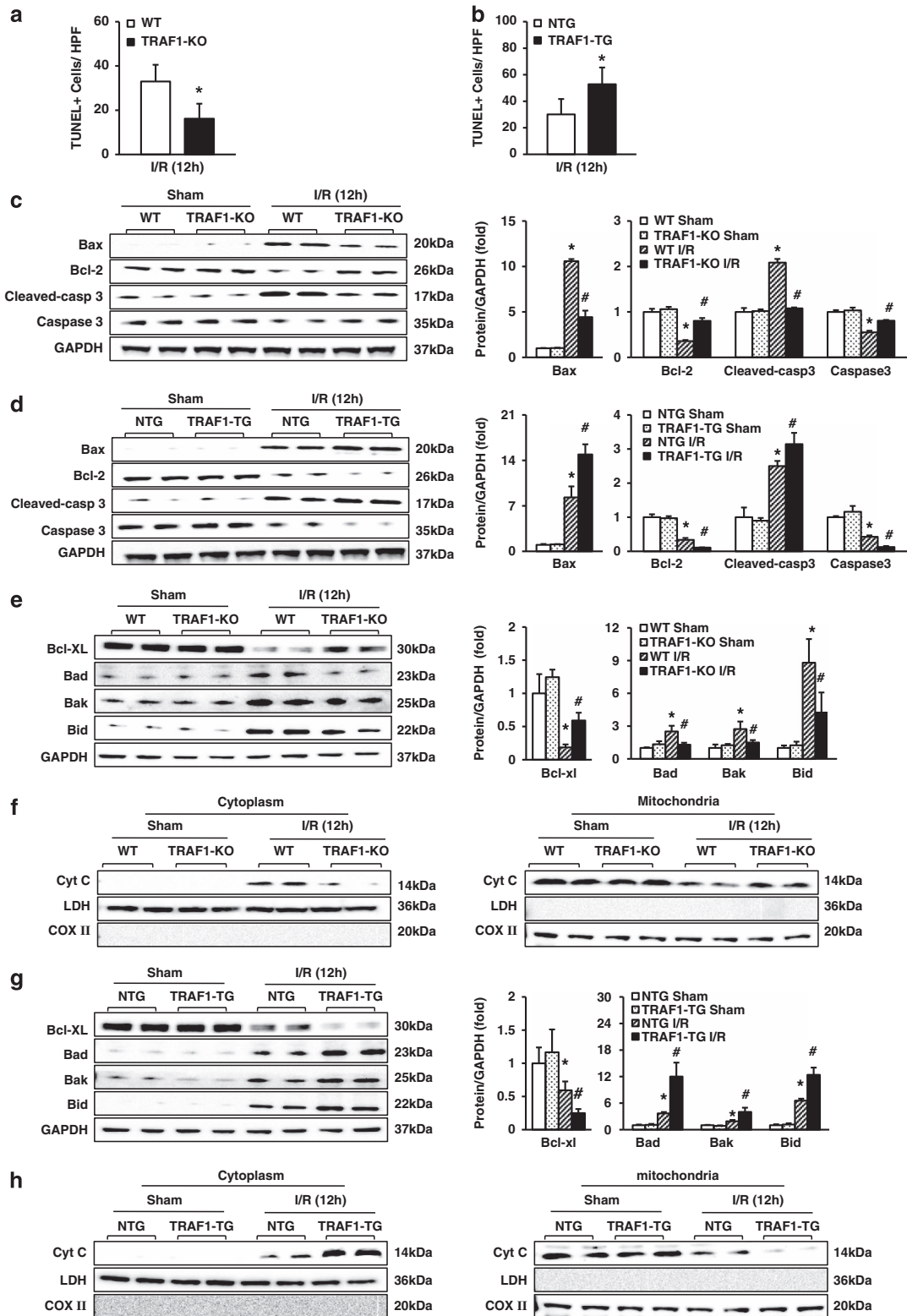


Figure 2 (Continued)



**Figure 3** TRAF1 deficiency blunts the inflammatory insult induced by I/R injury. (a) Quantification of serum MPO activity at the indicated time points after I/R ( $n = 8$  at each time point,  $*P < 0.05$  versus sham,  $\#P < 0.05$  versus I/R). (b) Fluorescence staining of the indicated protein (red) and nuclei (DAPI, blue) in the hepatic cells of mice after 12 h liver I/R. Scale bar: 20  $\mu$ m. (c) Quantification of the indicated protein-positive cells ( $n = 5-13$ ,  $*P < 0.05$  versus WT or NTG). (d) Flow cytometry analysis of isolated cells from ischemic liver lobes stained with CD11b and either of anti-F4/80, Ly6G and Ly6C antibodies. (e, f) Quantification of the mRNA levels of TNF- $\alpha$ , IFN $\gamma$ , IL-1 $\beta$ , IL-2, IL-6, and IL-10 in WT and TRAF1-KO mice, and NTG and TRAF1 TG mice, 12 h after sham surgery or I/R ( $n = 6$  or 9,  $*P < 0.05$  versus sham,  $\#P < 0.05$  versus I/R). (g, h) Quantification of the protein levels of TNF- $\alpha$ , IL-1 $\beta$ , IL-2, IL-6, and IL-10 in the peripheral blood of indicated mice 12 h after sham surgery or I/R ( $n = 7$  or 8,  $*P < 0.05$  versus sham,  $\#P < 0.05$  versus I/R). (i, j) Western blot analysis of the indicated proteins in hepatic tissues from WT/TRAF1-KO mice and NTG/TRAF1 TG mice after sham surgery or 12 h I/R ( $n = 6$ ,  $*P < 0.05$  versus sham,  $\#P < 0.05$  versus I/R). GAPDH served as a loading control. Data are presented as the mean  $\pm$  S.D.



**Figure 4** TRAF1 mediates I/R-induced cell death. (a, b) Quantification of TUNEL-positive cells of WT and TRAF1 KO (a), and NTG and TRAF1 TG (b) mice after 12 h I/R ( $n = 7-13$ ,  $*P < 0.05$  versus WT or NTG). (c, d, e, g) Western blot analysis of the indicated proteins in the hepatic tissues of WT/TRAF1 KO (c, e) and NTG/TRAF1 TG (d, g) mice after sham surgery or 12 h I/R injury. The right panels indicate the quantification of these proteins ( $n = 6$ ,  $*P < 0.05$  versus sham,  $\#P < 0.05$  versus I/R). Data are presented as the mean  $\pm$  S.D. (f, h) Release of cytochrome c (Cyt C) from mitochondria into the cytoplasm of hepatic cells from WT/TRAF1 KO (f) and NTG/TRAF1 TG (h) mice. LDH and COX II are shown as the internal markers for cytoplasm and mitochondria, respectively. LDH, lactate dehydrogenase; COX II, cytochrome c oxidase subunit II

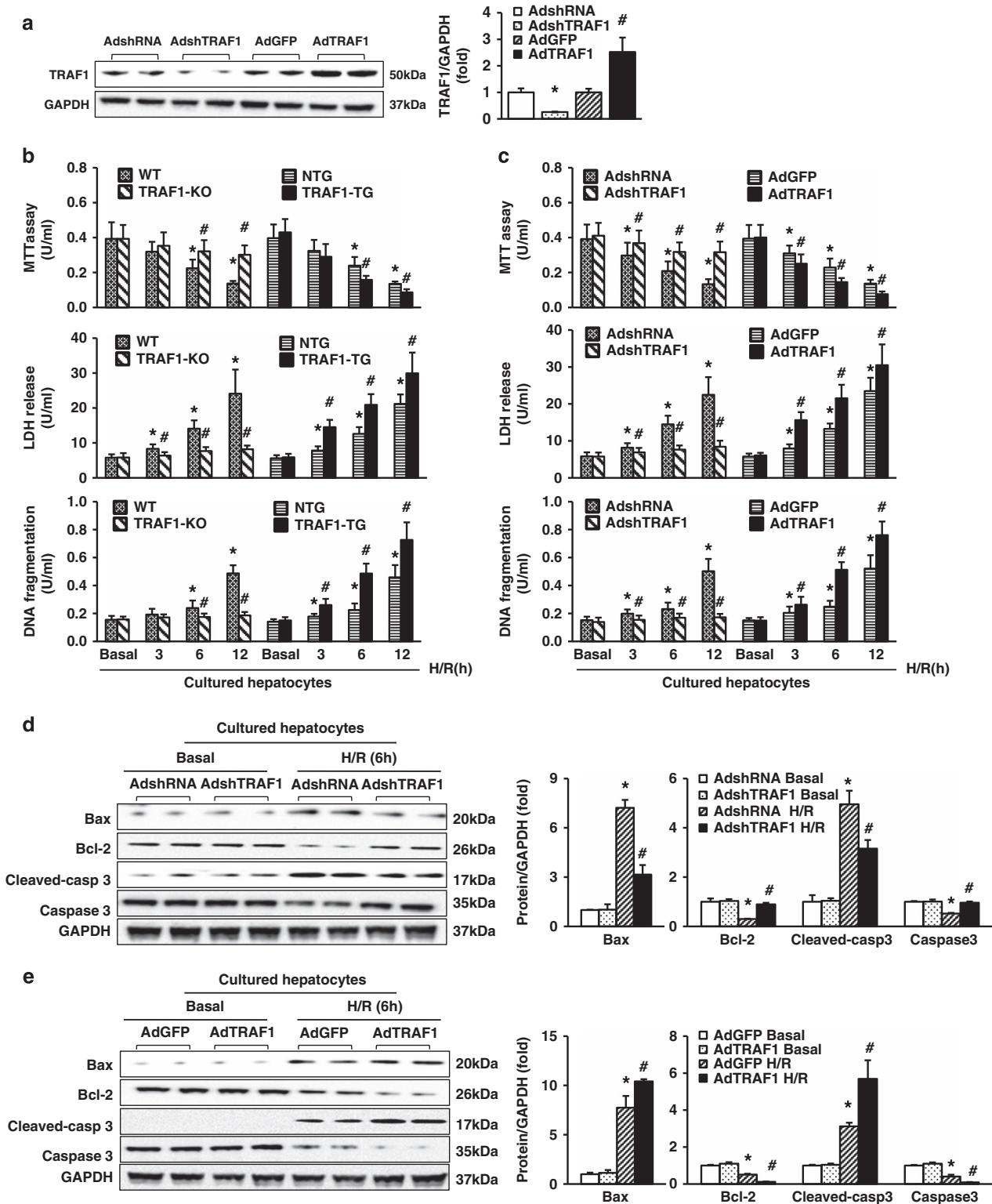


**Figure 5** TRAF1 is a modulator of hepatocyte survival after H/R. (a) Western blot analysis of TRAF1 expression in cultured hepatocytes infected with the indicated adenovirus (left) and the quantification of TRAF1 normalized to GAPDH. ( $n=4$ , \* $P<0.05$  versus AdshRNA, # $P<0.05$  versus AdGFP). (b) Cell viability, LDH release and DNA fragmentation of hepatic cells isolated from WT/TRAF1 KO and NTG/TRAF1 TG mice at the indicated time points after H/R. ( $n=11$  or  $12$  for each time point, \* $P<0.05$  versus Basal, # $P<0.05$  versus H/R). (c) Cell viability, LDH release and DNA fragmentation of primary hepatocytes infected with AdshRNA/AdshTRAF1 and AdGFP/AdTRAF1 at the indicated time points after H/R ( $n=12$  for each time point, \* $P<0.05$  versus Basal, # $P<0.05$  versus H/R). (d, e) Western blot analysis of apoptosis-related protein levels in cells infected with the indicated adenoviral vectors for 48 h and subjected to H/R for 6 h. Right panel: quantification of protein levels ( $n=6$ , \* $P<0.05$  versus AdshRNA or AdGFP control, # $P<0.05$  versus AdshRNA or AdGFP H/R). Data are presented as the mean  $\pm$  S.D.



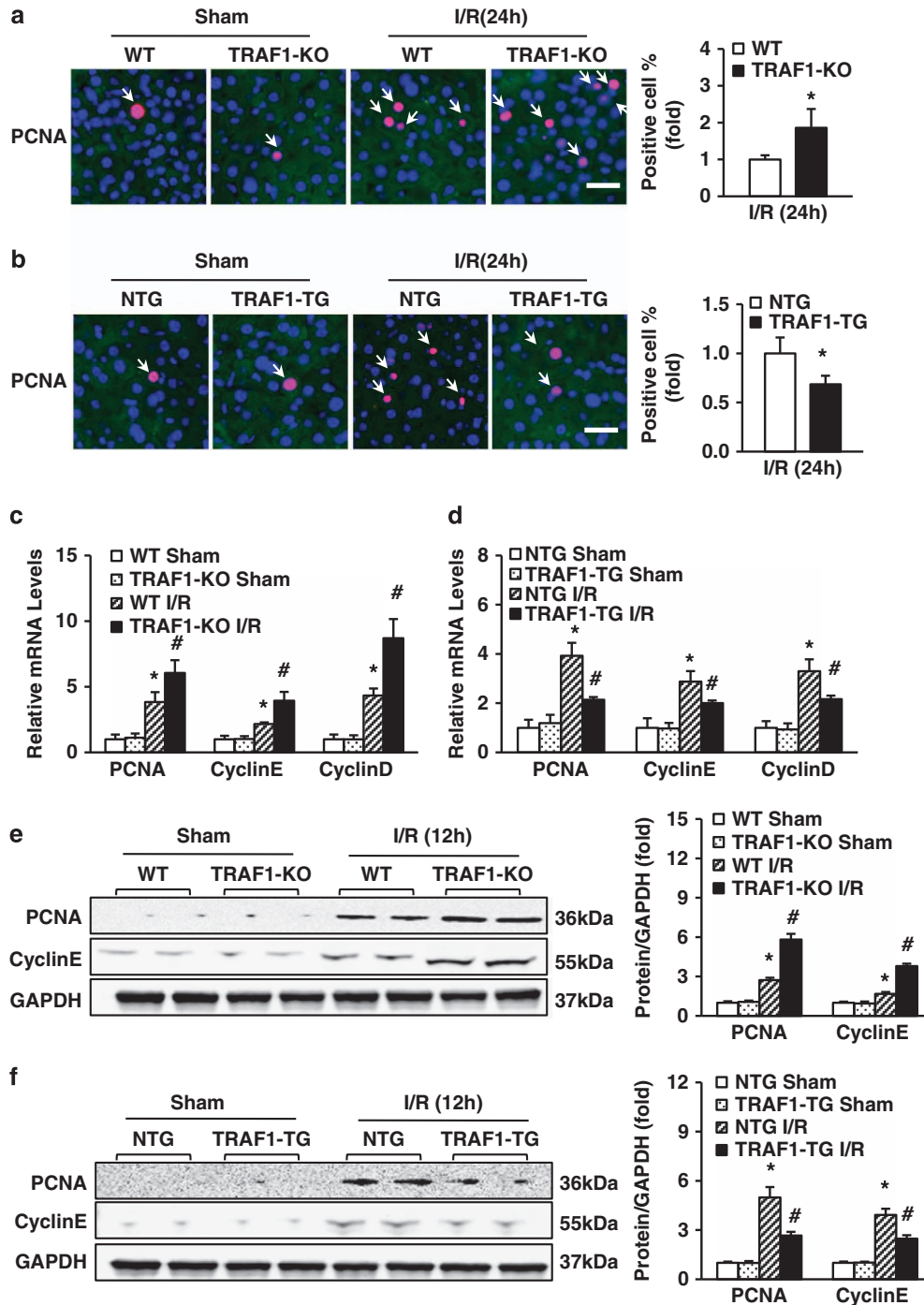


**Figure 6** TRAF1 regulates the regenerative capacity of the liver. (a, b) Fluorescence staining of PCNA (red) and nuclei (DAPI, blue) in the hepatic cells of WT/TRAF1 KO (a) and NTG/TRAF1 TG (b) after sham surgery or 24 h liver I/R. Scale bar: 20  $\mu$ m. The right panels demonstrate the quantification of PCNA-positive cells ( $n=10-20$ , \* $P<0.05$  versus WT/NTG). (c, d) Quantification of the mRNA levels of PCNA, cyclin D, and cyclin E in WT/TRAF1 KO (c) and NTG/TRAF1 TG (d) mice after sham surgery or 24 h liver I/R ( $n=9$ , \* $P<0.05$  versus sham, # $P<0.05$  versus I/R). Data are presented as the mean  $\pm$  S.D. (e, f) Western blot analysis of the levels of PCNA and cyclin E in hepatic cells of WT and TRAF1 KO (e) and NTG and TRAF1 TG (f) mice after sham operation or 12 h liver I/R. Right panel: quantification of protein levels ( $n=6$ , \* $P<0.05$  versus sham, # $P<0.05$  versus I/R). Data are presented as the mean  $\pm$  S.D.

using western blot analysis, and observed that basal phosphorylation of ASK1 in liver tissue was low and that ASK1 phosphorylation was increased 12 h after I/R (Figures 7a and b). Notably, the phosphorylation of ASK1 was markedly decreased to basal levels in TRAF1-deficient liver

tissue after I/R (Figure 7a). Once activated, ASK1 phosphorylates the MAPK kinases MKK4/7 and MKK3/6, which in turn promote JNK and p38 kinase activities, respectively.<sup>27</sup> For the stress-type specificity of MAP kinase kinases, we sought to investigate downstream components of the liver

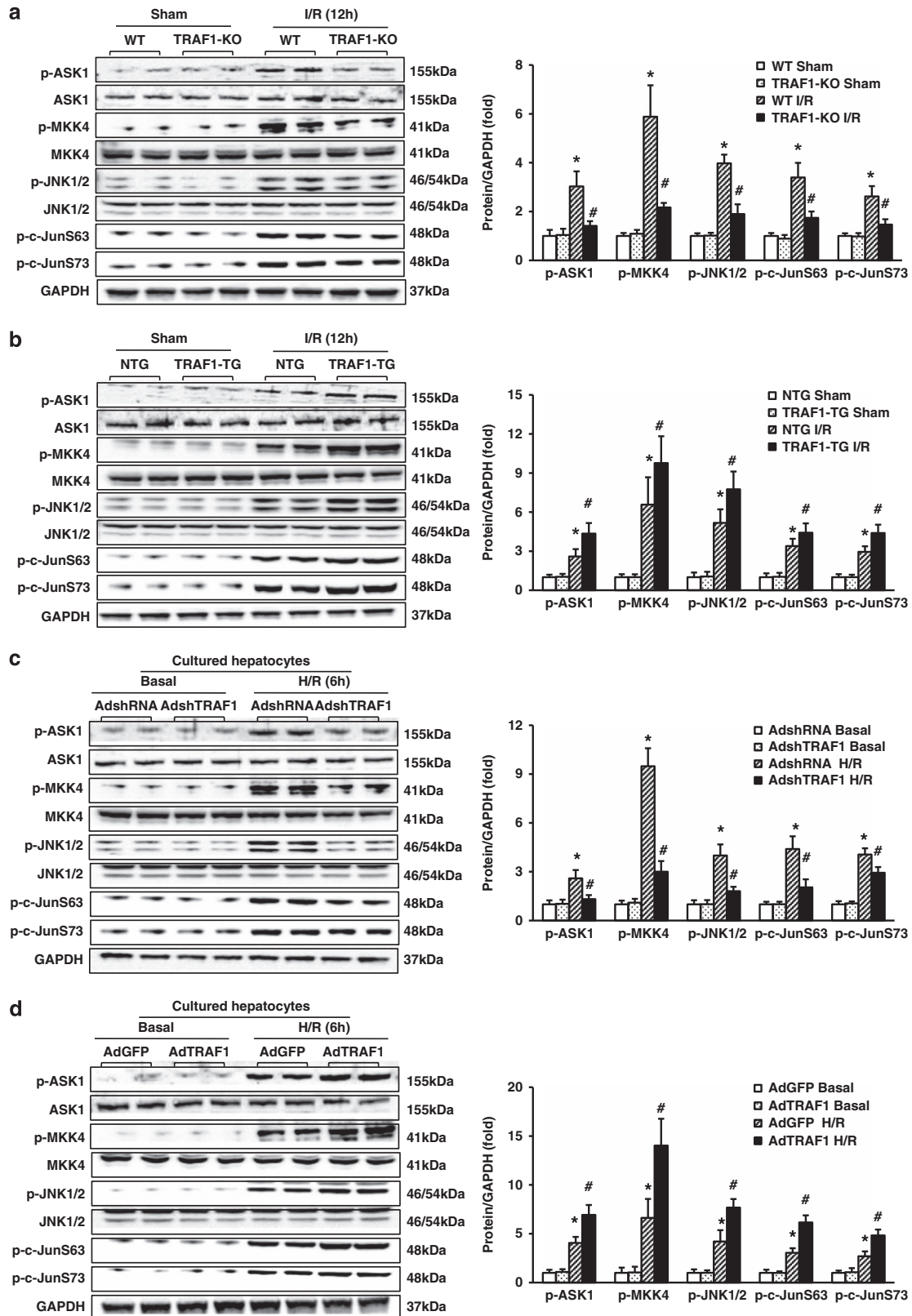


**Figure 7** TRAF1 has an important role in the activation of the ASK1-MKK4-JNK signaling pathway. (a, b) Western blot analysis (left) and quantification (right) of the levels of the indicated proteins in the hepatic tissues of WT/TRAF1 KO (a) and NTG/TRAF1 TG (b) mice after sham surgery or 12 h liver I/R ( $n=6$ ,  $*P<0.05$  versus sham,  $\#P<0.05$  versus I/R). (c, d) Western blot analysis (left) and quantification (right) of the levels of the indicated proteins in hepatocytes infected with the indicated adenovirus for 48 h and subjected to H/R for 6 h ( $n=6$ ,  $*P<0.05$  versus AdshRNA or AdGFP control,  $\#P<0.05$  versus AdshRNA or AdGFP H/R). GAPDH served as an internal control. Data are presented as the mean  $\pm$  S.D.

I/R-responsive pathway(s). Using a western blotting screen, we observed that the phosphorylation of MKK4 and JNK induced by I/R was also lower in the absence of TRAF1 (Figure 7a), although the total protein levels of these kinases were not altered in TRAF1-KO and WT groups. In parallel, the level of phosphorylated c-Jun (at the Ser63 and Ser73 residues) was markedly increased by liver I/R, but this increase was inhibited in the liver of TRAF1-KO mice (Figure 7a). In contrast, the phosphorylation levels of each member of the ASK1-MKK4-JNK-c-Jun pathway were significantly increased in TRAF1-overexpressing livers after I/R challenge, although no difference was observed between the TRAF1 TG and NTG control groups under sham operation conditions (Figure 7b).

We therefore hypothesized that the effect of TRAF1 on the MAPKKK signaling pathway may have occurred in hepatic parenchymal cells. Consistent with the *in vivo* results, after H/R treatment, cultured hepatocytes exhibited higher protein levels of phosphorylated ASK1, MKK4, JNK, and c-Jun (Figures 7c and d). As expected, the amount of these phosphorylated proteins was lower in cells that had been transfected with AdshTRAF1 under H/R conditions but was higher in hepatocytes transfected with AdTRAF1 (Figures 7c and d).

**TRAF1 physically interacts with ASK1.** As the TRAF2 and TRAF6 proteins have been shown to be recruited to ASK1, we sought to determine whether TRAF1 can also bind to ASK1. HepG2 cells were transfected with Flag-tagged ASK1 and Myc-tagged TRAF1, and the protein–protein interactions were assessed by immunoprecipitation (IP). We observed obvious binding of TRAF1 to ASK1 in this *in vitro* system (Figure 8a), demonstrating that the interaction is direct. Furthermore, primary hepatocytes were lysated for IP with either TRAF1-specific antibody or ASK1-specific antibody, and endogenous TRAF1 and ASK1 were also found to interact in this system (Figure 8b).

To determine the interaction regions, deletion mutants of TRAF1 and ASK1 were constructed and analyzed for their ability to interact with each other (Figure 8c). HepG2 cells were co-transfected with full-length or truncated TRAF1 expression vectors with Myc tags and with Flag-tagged ASK1 expression vector. The cell lysates were immunoprecipitated with anti-Myc or an anti-Flag antibody and then analyzed by western blotting using anti-Flag or anti-Myc antibody, respectively. The results showed that residues 188–409 of TRAF1 were responsible for the interaction (Figures 8d and f). Similarly, we co-transfected HepG2 cells with a series of Flag-tagged ASK1 constructs and full-length Myc-tagged TRAF1 and performed IP, and we confirmed that only the construct consisting of ASK1 C terminus (residues 941–1375) lost the ability to bind to TRAF1 (Figures 8e and g), indicating that all of the other ASK1 domains contributed to this interaction.

To investigate the putative relationship between TRAF1 and ASK1, we investigated whether TRAF1 colocalizes with ASK1 *in vitro*. HepG2 cells were co-transfected with GFP-fusion proteins of full-length TRAF1 or the TRAF1 N terminus (residues 1–187) and a mCherry-fusion protein of ASK1. The subcellular localization of the proteins was visualized by confocal microscopy and image processing. Full-length

TRAF1 and the N terminus of TRAF1 were perfectly colocalized with ASK1 in the cytoplasm, although the TRAF1 N terminus was unable to interact with ASK1 *in vitro*. (Figure 8h). To further confirm the TRAF1–ASK1 interaction *in vivo*, we used fluorescence resonance energy transfer (FRET), in which the energy transfer between the donor and acceptor depends on the distance and dipole orientations of the two partners. We co-transfected 293T cells with vectors expressing CFP-fused ASK1 and YFP-fused full-length TRAF1 or TRAF1 N terminus (residues 1–187) as the donor–acceptor pair. To measure FRET in cells, we used the dequenching approach in which the mean fluorescence intensities of the donor (CFP) fluorophores were recorded before and after acceptor (YFP) photobleaching. The average FRET efficiency was calculated, and the intensities of ASK1-CFP fluorescence increased by 8.69% with coexpressed full-length TRAF1-YFP, but only by 1.64% with coexpressed truncated TRAF1. The detected FRET suggests that the C-terminal domain of TRAF1 is required for the association of the two proteins (Figures 8i and j).

**The kinase activity of ASK1 is crucial for its function in hepatocytes.** Owing to the direct interaction of TRAF1 with ASK1 and the observation that the levels of phosphorylated ASK1 were lower in TRAF1-deficient mice, we hypothesized that the inhibition of the physical binding between TRAF1 and ASK1 blocks the effect of TRAF1 on ischemic hepatocytes. We then constructed recombinant adenoviruses expressing mutant ASK1 that could not bind to TRAF1. Transfection of cultured hepatocytes with the vector carrying this mutant ASK1 did not increase the H/R-induced cell damage, as measured by an MTT assay and an LDH release assay (Figure 8k), indicating that the dissociation of ASK1 from TRAF1 eliminates the damage caused by excessive wild-type TRAF1.

We transfected TRAF1-deficient hepatocytes with AdASK1 and observed that the overexpression of ASK1 exacerbated the cell injury, abrogating the hepatoprotective effect of targeting TRAF1 (Figure 8l). Finally, we examined whether the activity of ASK1 is required for its effect on hepatocyte survival. Accordingly, hepatocytes isolated from TRAF1 TG or NTG mice were transfected with adenoviruses expressing dominant-negative ASK1 (Addn-ASK1). Surprisingly, higher MTT values and less LDH release were observed in the Addn-ASK group, indicating that H/R-induced cell injury was suppressed by dnASK1 (Figure 8m). The above data demonstrated that TRAF1–ASK1 signaling has an important role in I/R-associated hepatocyte injury.

## Discussion

TNF- $\alpha$  participates in liver I/R injury by modulating both the inflammatory response and cell death,<sup>28</sup> however, the understanding of TNF- $\alpha$ -mediated signal transduction during liver I/R is limited.<sup>28,29</sup> In the current study, we sought to determine how TRAF1, a key molecule in the TNF pathway,<sup>17</sup> is involved in hepatic I/R. We demonstrated for the first time that TRAF1 expression is upregulated in the liver following warm I/R injury. Furthermore, we demonstrated that increased TRAF1 expression contributes to hepatic damage, whereas TRAF1 deficiency provides resistance to I/R injury.

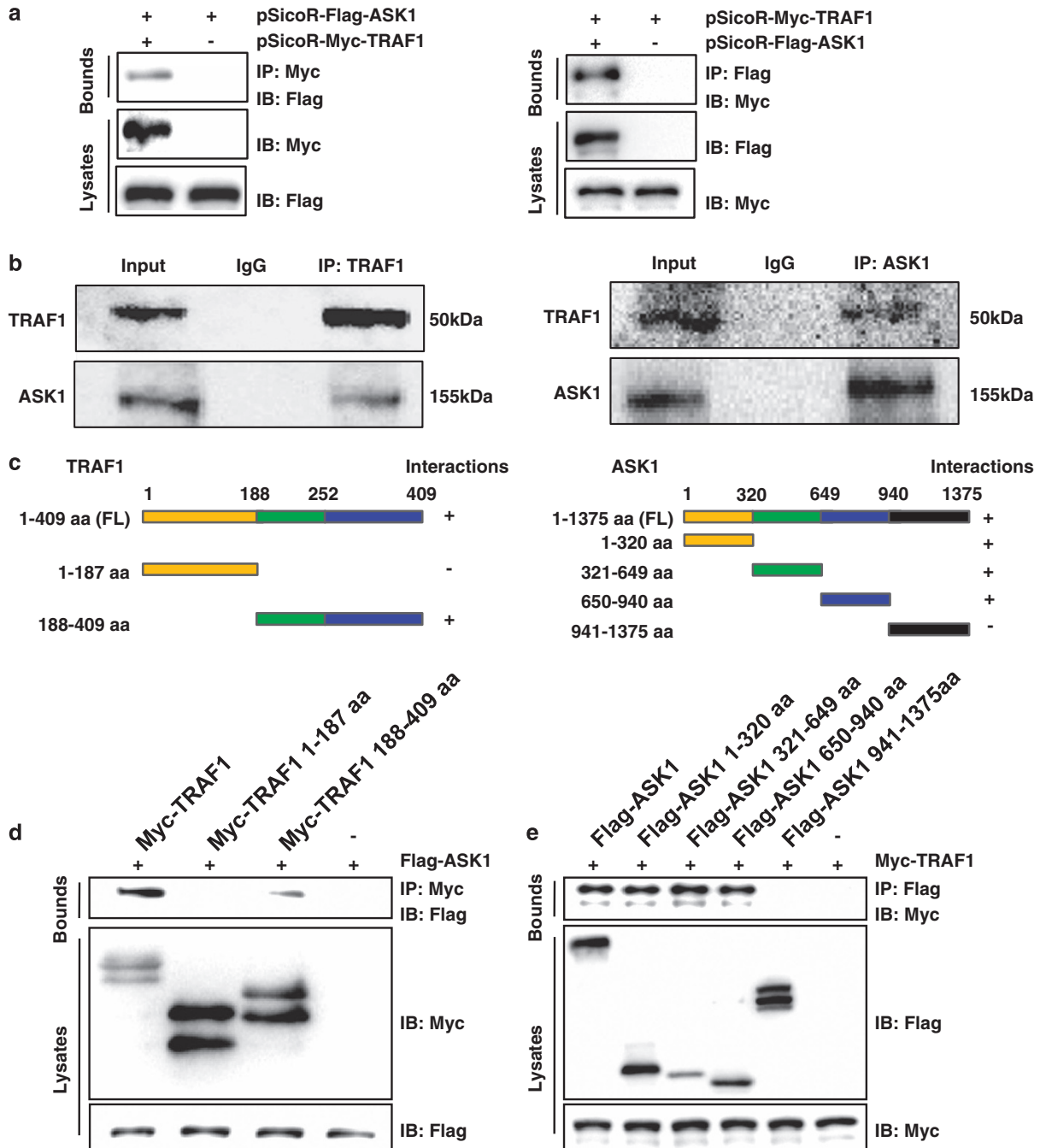


**Figure 8** TRAF1 function is ASK1-dependent during liver I/R injury. (a) Co-immunoprecipitation of TRAF1 and ASK1 from HepG2 cells transfected with Myc-tagged TRAF1 and Flag-tagged ASK1. The lysates were immunoprecipitated with anti-Myc (left) or anti-Flag (right) antibody and analyzed by immunoblotting as indicated. (b) The interaction of endogenous TRAF1 and ASK1 detected by co-immunoprecipitation. (c) Schematic representation of the TRAF1 and ASK1 deletion mutants. (d, f) Mapping of the ASK1-binding region of TRAF1. HepG2 cells were transfected with Flag-tagged ASK1 and Myc-tagged TRAF1 mutants or control vector. The lysates were immunoprecipitated with anti-Myc (d) or anti-Flag (f) antibody and immunoblotted with the indicated antibodies. (e, g) Mapping of the TRAF1-binding region of ASK1. HepG2 cells were transfected with Myc-tagged TRAF1 and Flag-tagged ASK1 mutants or control vector. The lysates were immunoprecipitated with anti-Flag (e) or anti-Myc (g) antibody and immunoblotted as indicated. (h) Colocalization of full-length (1–409 aa) or truncated (1–187 aa) EGFP-TRAF1 and mCherry-ASK1 in the cytoplasm of HepG2 cells. (i) ASK1-CFP and full-length (1–409 aa) or truncated (1–187 aa) TRAF1-YFP fluorescence with excitation/emission at 457/485 nm (top) and 514/535 nm (bottom). (j) The average efficiency after photobleaching is indicative of the FRET occurring between ASK1-CFP and TRAF1-YFP ( $n = 4$ ,  $\#P < 0.05$ ). (k) Quantification of cell viability and LDH release of cultured hepatocytes infected with AdGFP, AdTRAF1, or an Ad-mutant harboring a mutant TRAF1-domain and subjected to H/R for 12 h ( $n = 12$ , NS, not significant). (l, m) Quantification of cell viability and LDH release of primary hepatocytes isolated from WT/TRAF1 KO (l) and NTG/TRAF1 TG mice (m) infected with AdGFP, AdASK1 and Addn-ASK1 and subjected to H/R for 12 h ( $n = 12$ , NS, not significant)



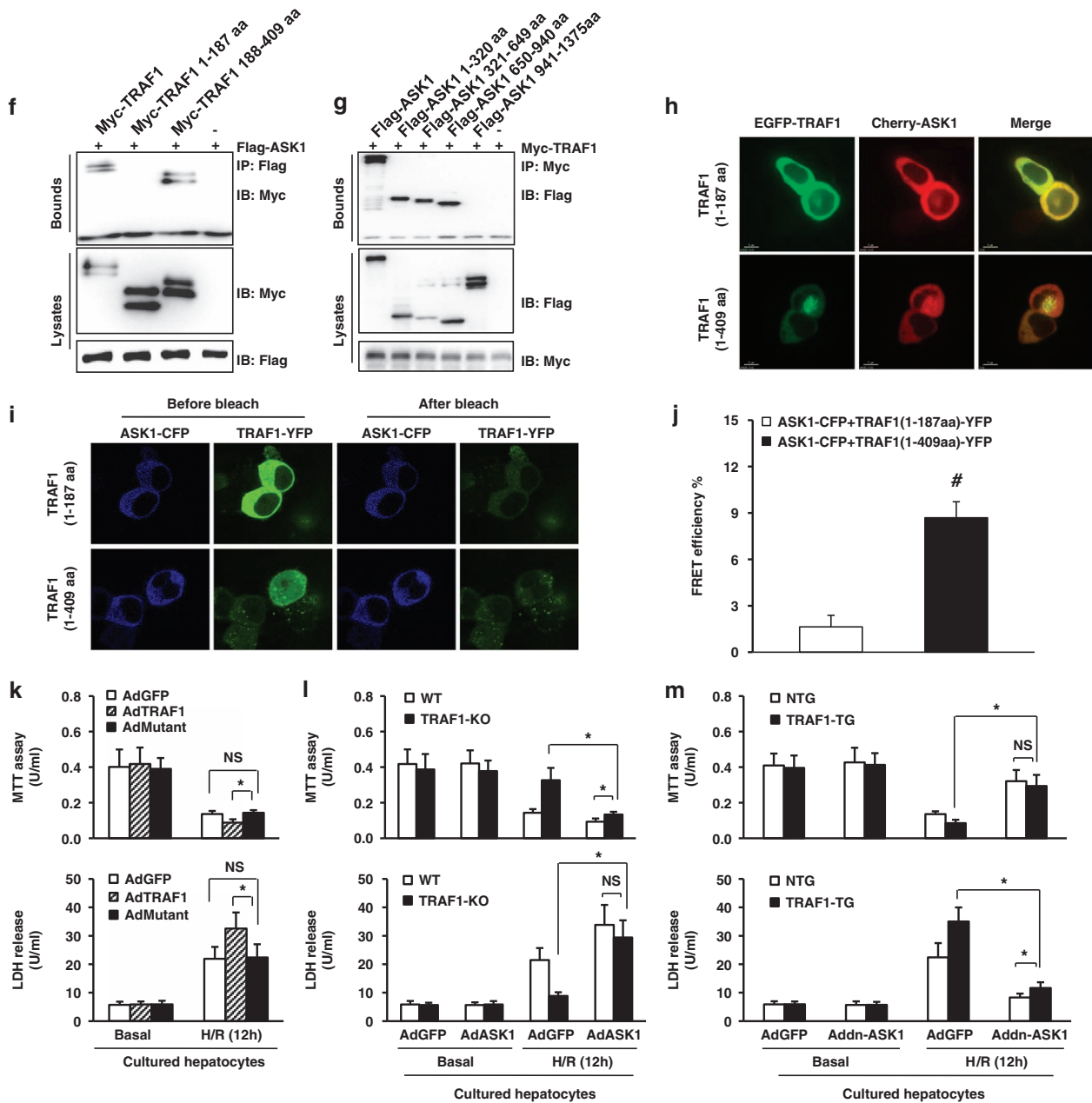


Figure 8 (Continued)

Hepatic I/R results in TNF- $\alpha$  production by immune cells, which is correlated with the severity of liver injury.<sup>30</sup> In addition, hepatocytes have been shown to exhibit higher TNFR expression levels in acute and chronic inflammatory liver diseases.<sup>31</sup> TNF- $\alpha$  binds to its receptors, inducing receptor oligomerization and the association of various adapter proteins, including TRAF1.<sup>32</sup> We hypothesized that TRAF1 also regulated in ischemic liver diseases. Previous reports have demonstrated that TRAF1 is expressed in lymphocytes, dendritic cells, and certain epithelia but not in the liver.<sup>11,16</sup> In this study, we provide evidence that in the normal liver, TRAF1 expression is low, but after hepatic I/R TRAF1 mRNA and protein levels are significantly higher than in mice subjected to sham operation. Similarly, hepatocytes exposed to H/R exhibit

high TRAF1 expression. We hypothesized that hepatic TRAF1 is strongly upregulated in response to TNF- $\alpha$  activation after reperfusion; however, we observed only a slight induction of TRAF1 after 60 min of ischemia, and this induction may have been caused by other, unknown, mechanisms. Intratracheal administration of TNF- $\alpha$  did not induce TRAF1 in hepatocytes;<sup>33</sup> thus, we believe that the hepatic TRAF1 upregulation after I/R depends on the context or stressor type.

TRAF1 is transcriptionally upregulated by TNF- $\alpha$  and other ligands and has an inhibitory function in special processes.<sup>12,17-19</sup> Unexpectedly, the increased expression of TRAF1 appeared to promote the inflammatory pathophysiology of hepatic I/R injury in our study. The hepatocyte-specific TRAF1-overexpressing mice exhibited significantly

higher aminotransferase levels and more severe necrosis. Strikingly, the number of infiltrating immune cells and the levels of local or circulating pro-inflammatory cytokines were higher in TRAF1 TG mice. In contrast, TRAF1 knockout resulted in significantly reduced inflammation, with lower levels of pro-inflammatory cytokines and less immune cell infiltration. The inflammatory response mediated by a number of cytokines/chemokines released by infiltrating leukocytes or parenchymal cells has been considered to promote most of the tissue damage apart from the initial cellular injury, which is directly caused by ischemia.<sup>22,29</sup> Therefore, the effect of TRAF1 on hepatic damage appears to be at least partially due to its potential to regulate the immune response.

TRAF1 exerts diverse and often conflicting biological effects that are dependent on cell type and context.<sup>15,16</sup> Our findings of the protective function of TRAF1 KO on liver injury induced by warm I/R appear to be incompatible with the results from another model in which TRAF1-KO mice treated intratracheally with TNF- $\alpha$  exhibited markedly more liver injury than WT mice.<sup>33</sup> In the present study, hepatocyte TRAF1 was a deleterious factor, promoting inflammation and TNF- $\alpha$  under the I/R-induced stress. A recent report identified TRAF1 as a pro-inflammatory mediator of atherosclerosis, a chronic inflammatory disease,<sup>34</sup> which is consistent with our findings and supports the hypothesis that TRAF1-mediated function depends on the cell type or disease.

TRAF1 has been reported to be a regulator of cell fate that suppresses TNF- $\alpha$ -mediated apoptosis.<sup>35</sup> In another previous study, TRAF1-deficient T cells markedly proliferated after TNF treatment, and TNF-induced skin necrosis was exacerbated in TRAF1-null mice.<sup>19</sup> However, these results mostly revealed the effect of TRAF1 after TNF- $\alpha$  administration, and little is known about the response under other stresses. Our study demonstrated that in addition to inhibiting inflammation, TRAF1 deficiency also attenuates cell death and enhances the regeneration of hepatocytes after liver I/R, which is in contrast to the prevalent opinion that TRAF1 exhibits antiapoptotic functions.<sup>35,36</sup> TRAF1 functioned as a proapoptotic gene in hepatocytes in our warm liver I/R model, and TRAF1 functioned in both the ischemia and the reperfusion phases.

ASK1 is well known to have a pivotal role in oxidative stress-induced cell death,<sup>37</sup> and TRAF2 and TRAF6 bind to and activate ASK1 to promote cell death.<sup>38</sup> In this study, we demonstrated that TRAF1 can interact with ASK1 and increase the phosphorylation level of ASK1, suggesting a novel signaling mechanism involving TRAF family proteins and ASK1 in I/R-induced cell death.

Similar to other TRAF family members, TRAF1 has a conserved C-terminal TRAF domain that is responsible for its association with TNFR cytoplasmic tails and for its oligomerization.<sup>16</sup> The N terminus of TRAF1 lacks a RING domain, and therefore differs from all of the other TRAF adapter molecules.<sup>39</sup> Thus, the interaction between TRAF1 and ASK1 appears to be specific, and the C terminus of TRAF1 (TRAF domain) is required for the association. Although the binding domain of TRAF is present in the N terminus of ASK1,<sup>37</sup> the kinase domain of ASK1 is also crucial for binding to TRAF1, highlighting the uniqueness of this interaction.

ASK1 is autophosphorylated and activated in the hippocampus under ischemic stress.<sup>40</sup> We observed higher levels of phosphorylated ASK1 in the liver after I/R, and this increase in ASK1 phosphorylation was abrogated in the TRAF1-deficient liver and augmented in the TRAF1-overexpressing liver. Furthermore, the isolated hepatocytes exposed to H/R exhibited higher ASK1 phosphorylation. Adenovirus-mediated TRAF1 knockdown inhibited ASK1 phosphorylation, whereas ASK1 phosphorylation was markedly induced by TRAF1 overexpression. This evidence strongly suggests that ASK1 is activated by TRAF1 after I/R, although the mechanism is still not well understood.

JNK has been shown to be phosphorylated and activated by liver I/R injury,<sup>41</sup> and we also observed this in our liver I/R model. Moreover, the concurrent expression of phosphorylated ASK1, MKK4, JNK, and c-Jun was observed in the current study. The TRAF1-deficient livers exhibited lower levels of these phosphorylated signal transducers after hepatic I/R, whereas hepatic overexpression of TRAF1 exacerbated the activation of this signaling pathway, indicating that TRAF1 may regulate liver damage through the ASK1-MKK4-JNK pathway. Recently, the influence of the innate immune system and the interplay of the innate and adaptive immune systems in the pathogenesis of I/R injury were elucidated.<sup>42</sup> The present study provides novel evidence that TRAF1-deficient mice are resistant to liver I/R injury and demonstrates that TRAF1 deficiency has a protective effect on both the inflammatory response and cell death. Owing to the regulation of ASK1-MKK4-JNK signal transduction by TRAF1, the specific inhibition of TRAF1 and its downstream pathway may be a therapeutic target against the detrimental consequences of liver I/R.

#### Materials and Methods

**Animals.** All animal procedures were approved by the Animal Care and Use Committee of Renmin Hospital of Wuhan University. Animal experiments were performed in accordance with the National Institutes of Health Guide for the Care and Use of Laboratory Animals (NIH Publication No. 80-23 revised in 1996). TRAF1-KO mice (C57BL/6J background) were purchased from the Jackson Laboratory (Bar Harbor, ME, USA; Stock No. 008076), and the knockout was confirmed via PCR analysis using the primers 5'-GCCAGAGGCCACTTGTGTAG-3', 5'-CAGAACCCTTGCCTAATCC-3', and 5'-TCCTAGAGCCTGCTGCTAA-3'. To generate hepatocyte-specific TRAF1 TG mice, full-length murine TRAF1 cDNA amplified with the forward primer 5'-GAACTCGAGCCACCATGGCTCCAGCTCAGCCCC-3' and reverse primer 5'-GAAGGATCCTAAGCACTAGTGTCCCAA-3' was cloned downstream of the albumin promoter. This construct was microinjected into fertilized embryos (C57BL/6J background) to produce hepatocyte-specific TG mice, and four independent TG lines were established. Genomic DNA was extracted from the tail for genotyping using PCR analysis with the primers 5'-AAGGGTGGCAACTTCTCCTC-3' (forward) and 5'-ATAAGGAATGGACAGCAGGG-3' (reverse). Only 8- to 10-week-old (24–27 g) males were used. All mice were housed in an environment with controlled light (12 h light/dark), humidity, and temperature, with food and water available *ad libitum*.

**Mouse hepatic I/R injury model.** A non-lethal model of segmental (70%) warm hepatic I/R injury was performed after the mice were anesthetized by pentobarbital sodium (50 mg/kg, i.p., Sigma-Aldrich, P3761, St. Louis, MO, USA). First, a midline laparotomy was performed after the abdominal wall of the mice was shaved and cleaned with Betadine. An atraumatic microvascular clamp (Fine Science Tools, North Vancouver, BC, Canada) was used to occlude the vasculature supplying the left and median lobes (ischemic lobes) of the liver for 60 min. Evidence of ischemia was confirmed by visualizing the pale blanching of the ischemic lobes. The mice in whom no ischemic color changes were observed or who exhibited a lack

of response to reperfusion were immediately killed. The abdomen was covered during the ischemic period, and the body temperature of the mice was maintained at 36.5–37.5 °C through the use of a homeothermic blanket. After the removal of the clamp, reperfusion was confirmed by the color change of the ischemic lobes. Finally, the abdomen was closed with a continuous 4-0 polypropylene suture. Sham mice underwent the same surgical procedure without vasculature occlusion.

**Liver damage assessment.** The serum aspartate aminotransferase (sAST) and serum alanine aminotransferase (sALT) levels were determined by using a spectrophotometer (Chemix 180i, Sysmex, Shanghai, China). Liver MPO activity was measured in frozen tissues according to the published methods,<sup>43</sup> with slight modifications. In brief, 100 mg of liver tissue was homogenized in 2 ml of buffer containing 3.4 mmol/l of  $\text{KH}_2\text{HPO}_4$  and 16 mmol/l of  $\text{Na}_2\text{HPO}_4$  (PH 7.4). After the mixture was centrifuged for 20 min at 10 000 × g, the precipitation was resuspended in 10 volumes of the buffer, which contains 43.2 mmol/l of  $\text{KH}_2\text{HPO}_4$ , 10 mmol/l of EDTA, 6.5 mmol/l of  $\text{Na}_2\text{HPO}_4$ , and 0.5% hexadecyltrimethylammonium (pH 6.0), and the sample was sonicated for 10 s. The supernatant was reacted with 3,3',3,5'-tetramethylbenzidine after being heated at 60 °C for 2 h. Finally, the change in absorbance was read by a spectrophotometer at 655 nm. For histopathological analysis, hematoxylin and eosin (H&E) staining was performed after the liver tissues were fixed in 10% formalin, embedded in paraffin, and sectioned (5 μm per section). The percentage of necrotic area was estimated by random evaluation of five high-power fields (×200) for each H&E section.

**Cytokine measurement.** Serum TNF-α, IL-1β, IL-2, IL-6, and IL-10 cytokine levels were measured by a commercially available enzyme-linked immunosorbent assay kit (PeproTech, Rocky Hill, NJ, USA; RayBio, Norcross, GA, USA; Invitrogen, Camarillo, CA, USA). Additional details are included in the Supplementary Table 1.

**Analysis of apoptosis.** Apoptosis was evaluated by a TUNEL assay with the ApopTag Plus *In Situ* Apoptosis Fluorescein Detection Kit (EMD Millipore Corporation, S7111, Billerica, MA, USA) according to the manufacturer's instructions. A commercially available cell death detection enzyme-linked immunosorbent assay kit (11585045001, Roche Applied Science, Penzberg, Germany) was used to assess the DNA fragmentation in primary hepatocytes according to the manufacturer's instructions.

**Immunofluorescence staining.** Immunofluorescence staining was performed as described previously.<sup>44,45</sup> In brief, paraffin-embedded liver tissues were cut into 5-μm sections and processed for immunofluorescence staining. After a 5-minute high-pressure antigen retrieval process in sodium citrate buffer (100 ×, pH 6.0), liver sections were washed in PBS containing 10% goat serum for 1 h and incubated with the indicated primary antibodies at 4 °C overnight: rabbit anti-Mac1 (CD11b, 1 : 100 dilution, ab75476, Abcam, Cambridge, MA, USA), anti-CD3 (1 : 100 dilution, ab16669, Abcam); rat anti-Ly6G (1 : 100 dilution, 551459, BD Biosciences, San Jose, CA, USA) and mouse anti-PCNA (1 : 100 dilution, 2586, Cell Signaling Technology, Beverly, MA, USA). After washing with PBS, the sections were incubated with the appropriate secondary antibodies for 1 h at 37 °C. The secondary antibodies used included anti-mouse immunoglobulin G (IgG) Alexa Fluor 568 conjugate (Invitrogen), anti-rat IgG Alexa Fluor 568 conjugate, and goat anti-rabbit IgG Alexa Fluor 568 conjugate. The nuclei were stained with 4',6-diamidino-2-phenylindole (DAPI). Images were obtained using a fluorescence microscope (OLYMPUS DX51, Tokyo, Japan) and DP2-BSW software (version 2.2, Tokyo, Japan), and the images were analyzed with Image Pro Plus (version 6.0, Media Cybernetics, Rockville, MD, USA).

**Primary hepatocyte isolation and culture.** Primary hepatocytes were cultured according to the published methods,<sup>43</sup> with a slight modification. Liver perfusion medium (Invitrogen, 17701-038) was used to perfuse the livers *in situ* via the portal vein and was followed by liver digest medium (Invitrogen, 17703-034) after anesthetizing the mice with pentobarbital sodium. The liver was excised and minced in William's E medium (Life technologies, A12176-01, Grand Island, NY, USA). The cell suspension was mixed gently several times with a pipette and strained through a steel mesh sieve after removing the liver capsule. The dispersed hepatocytes were collected via centrifugation at 50 × g for 5 min at 4 °C and washed twice with William's E medium. Hepatocytes were isolated by Percoll separation and washed twice with William's E medium. The final pellet was resuspended in William's E medium. The hepatocytes were counted, and their viability was determined by trypan blue exclusion. The hepatocytes were cultured under normoxic conditions (air/5% CO<sub>2</sub>) for further experiments.

**Adenoviral infection and hypoxia-reoxygenation model *in vitro*.** Adenoviruses harboring sequences encoding mouse TRAF1 and a short hairpin RNA targeting TRAF1 (shTRAF1) were generated. The open reading frame (ORF) of mouse TRAF1 was purchased from OriGene (MG206422, Rockville, MD, USA) and subcloned into a pCMV6-AC-GFP shuttle vector. Recombinant adenoviruses were generated using an AdEasy vector kit (Stratagene, La Jolla, CA, USA). Inserts were cloned into the pShuttle-CMV vector. Plasmids were recombined with the pAdEasy backbone vector according to the manufacturer's instructions, and HEK293 cells were transfected with the vector using FuGENE transfection reagent (E2312, Roche, Indianapolis, IN, USA). Recombinant adenoviruses were plaque-purified, titrated to 109 PFU/ml, and verified by restriction digestion. To generate shTRAF1, the hairpin-forming oligonucleotides TRAF1-f, 5'-GATCCGCGTGTGTTGAGAACATTGTTCTCGAGAA CAATGTTCTCAAACACACGTTTTTACGCGTG-3' and TRAF1-r, 5'-AATTCACGC GTAAAAACGTTGTTGAGAACATTGTTCTCGAGAACAATGTTCTCAAACACAC GG-3' were synthesized, annealed, and subcloned into the shuttle vector distal to the U6 promoter. Recombinant adenovirus was generated using a similar process. Cultured hepatocytes were transfected with adenovirus at a multiplicity of infection (MOI) of 100 for 48 h. To establish an I/R model *in vitro*, cultured cells were washed twice with PBS before the addition of serum-free DMEM/F12 medium saturated with 95% N<sub>2</sub>/5% CO<sub>2</sub> at 37 °C. The culture plates were then transferred to an experimental hypoxia chamber in a saturated atmosphere of 95% N<sub>2</sub> and 5% CO<sub>2</sub> for 60 min. The medium was then replaced with fresh normal maintenance medium that had been warmed, and oxygenated, and the plates were returned to a 37 °C humidified incubator under normoxic conditions (air/5% CO<sub>2</sub>) for the indicated times. Cells exposed to normoxic medium for the same periods were used as controls.

**Flow cytometry.** Flow cytometry was performed to assess kupffer cell, inflammatory monocyte, and neutrophil infiltration into the liver. In brief, ischemia liver lobes were aseptically collected from mice after 1 h of ischemia and 12 h of reperfusion and prepared as a single-cell suspension. Nonparenchymal cells (NPCs) were isolated from ischemic lobes (I/R) after 12 h of reperfusion. Groups were pooled and analyzed by flow cytometry as described previously.<sup>46</sup> We defined neutrophils as CD11bhiLy6Ghi, inflammatory monocytes as CD11bintLy6Chi, and Kupffer cells as CD11b+F4/80+. Antibodies were purchased from Biologend (San Diego, CA, USA): CD16/32 (clone 93), F4/80 (APC; clone BM8), Ly6G (PE; clone 1A8), Ly6C (FITC; clone HK1.4), CD11b (PerCP/Cy5.5; clone M1/70). Data were acquired with CyAn Advanced Digital Processing (ADP) analyzer (Beckman Coulter, Miami, FL, USA) and analyzed with Summit v4.2. Each experiment was repeated a minimum of three times.

**Quantitative real-time PCR and western blotting.** TRIzol Reagent (15596-026, Invitrogen) was used to isolate total RNA from the samples of liver tissue and primary hepatocytes. Two micrograms of total RNA was used for cDNA synthesis with the Transcriptor First Stand cDNA Synthesis Kit (04896866001, Roche). The differentially expressed genes were determined by quantitative real-time PCR using SYBR green (Roche, 04887352001), and the results were normalized using GAPDH expression. The primers used are presented in Supplementary Information (Supplementary Table 2). A western blot analysis was performed as previously described.<sup>44,45,47,48</sup> RIPA lysis buffer (720 μl RIPA, 20 μl PMSF, 100 μl Complete, 100 μl Phos-stop, 50 μl NaF, and 10 μl Na<sub>3</sub>VO<sub>4</sub> in 1 ml lysis buffer) was used to extract total protein from the liver tissue or cultured cells. The protein concentration was determined by the Pierce BCA Protein Assay Kit (Pierce, 23225, Rockford, IL, USA). Twenty micrograms of protein was resolved via 10% SDS-PAGE (Invitrogen, NP0301BOX) and then electrically transferred to a PVDF membrane (Millipore, IPVH00010, Billerica, MA, USA), which was blocked with TBS containing 5% skim milk powder for 90 min at room temperature. After incubation with the indicated primary antibody overnight at 4 °C, the membrane was incubated with a secondary peroxidase-conjugated antibody (Peroxidase-Affinipure Goat Anti-Mouse IgG (H+L) (115-035-003), Peroxidase-Affinipure Goat Anti-Rabbit IgG (H+L) (111-035-003), Jackson Immuno-Research Laboratories, Lincoln, NE, USA). Finally, a FluorChem E (Cell Biosciences, Santa Clara, CA, USA) imaging system was used for signal detection. Protein expression levels were quantified and normalized to the loading control GAPDH. All of the antibodies used in this study are listed in Supplementary Table 3.

**Assay of cell viability.** The MTT Cell Viability Assay Kit (11465007001, Roche) was used to determine cell viability, and lactate dehydrogenase (LDH) release was assessed by a colorimetric LDH cytotoxicity assay (G1782, Promega, Madison, WI, USA) according to the manufacturer's protocol.



**Plasmid constructs.** The mouse TRAF1 CDS was PCR amplified with TRAF1-5' and TRAF1-3' primers, digested with *Bam*HI and *Xho*I, and ligated into pSicoR-EGFP-myc digested with *Bam*HI and *Xho*I to create the EGFP-myc-TRAF1 recombinant. To obtain TRAF1 fragments consisting of residues 1 to 187 and 188 to 409, EGFP-myc-TRAF1 was PCR-amplified with TRAF1-5' and TRAF1-N-3' primers and the TRAF1-C-5' and TRAF1-3' primers, respectively. The products were digested with *Bam*HI and *Xho*I and ligated into pSicoR-EGFP-myc to create an in-frame fusion with EGFP-myc. Human ASK1 CDS was amplified with the ASK1-5' and ASK1-3' primers, digested with *Sal*I, and ligated into pSicoR-Flag-Cherry digested with *Xho*I to construct the Flag-Cherry-ASK1 recombinant. To obtain ASK1 fragments consisting of residues 1 to 320, 321 to 649, 650 to 940 and 940 to 1375, Flag-Cherry-ASK1 was PCR-amplified with the ASK1-5' and ASK1-N1-3' primers, the ASK1-N2-5' and ASK1-N2-3' primers, the ASK1-K-5' and ASK1-K-3' primers, and the ASK1-C-5' and ASK1-3' primers, respectively. The products were digested with *Bam*HI and *Sal*I, *Bam*HI and *Sal*I, *Bam*HI and *Sal*I or *Bgl*II and *Sal*I, respectively, and ligated into the pSicoR-Flag-Cherry digested with *Bam*HI and *Xho*I to create an in-frame fusion with Flag-cherry. The primers for making these constructs are presented in Supplementary Table S2. All plasmids were verified by sequencing.

**Immunoprecipitation.** Transient transfections of HepG2 cells with pSicoR-myc-TRAF1 and pSicoR-Flag-ASK1 into HepG2 cells were performed using FuGENE transfection reagent according to the manufacturer's instructions (Roche). After 48 h of incubation, the cells were lysed in ice-cold IP buffer (20 mM Tris-HCl, pH 8.0, 100 mM NaCl, 1 mM EDTA, and 0.5% NP-40) containing a protease inhibitor cocktail (Roche). For co-immunoprecipitation experiments, 500–1000  $\mu$ g of cell lysates was precleared with 10  $\mu$ l of protein A/G-agarose beads (11719394001, 11719386001, Roche) and immunoprecipitated with the indicated antibody with protein A/G-agarose beads. After 4 h of incubation at 4 °C, the beads were washed 5–6 times with 800  $\mu$ l of cold IP buffer, resuspended in 1  $\times$  loading buffer, and heated at 95 °C for 5 min. The cell lysates and immunoprecipitates were analyzed by western blotting as described above.

**Confocal microscopy.** HepG2 cells were seeded onto coverslips in 24-well plates. After co-transfection of pCherry-ASK1 and pEGFP-TRAF1 for 48 h, the cells were fixed with 4% fresh paraformaldehyde for 15 min, permeabilized with 0.2% Triton X-100 in PBS for 5 min, and stained with 1 g/ml DAPI for 15 min. Between each step, the coverslips were washed three times with 1  $\times$  PBS. The coverslips were removed from the wells and placed on a slide with mounting solution (D2522, Sigma). Images were acquired with an Olympus FV1000 confocal microscope.

**FRET.** For FRET, the TRAF1 (1–187 aa/1–409 aa) and ASK1 genes were cloned into pEYFP-N1 and pECFP-N1 as *Eco*RI-*Bam*HI fragments. The following PCR primers were used: for TRAF1 (1–187 aa), sense: 5'-ATGGCCTCCAGCTCAGCCCT-3'; anti-sense: 5'-CTAAGCACTAGTGTCACAA-3'; for TRAF1 (1–409aa), sense: 5'-ATGGCCTCCAGCTCAGCCCT-3'; anti-sense: 5'-CTAAGCACTAGTGTCACAATGC-3'; and for ASK1, sense: 5'-ATGAGCAGGAGGCGGACGA-3'; anti-sense: 5'-TCAAGTCTGTTGTTTCGAAA-3'. For FRET analysis, 293T cells ( $4 \times 10^6$  cells/100 mm dish) were co-transfected with ECFP-ASK1 and EYFP-TRAF1 (1–187 aa/1–409 aa) expression plasmids. CFP-ASK1 and YFP-TRAF1 were used as the donor-acceptor FRET pair. FRET was detected using the donor dequenching approach in which CFP fluorescence was measured before and after photobleaching of the YFP. The percentage dequenching FRET efficiency was calculated as  $E = (DQ - Q/DQ) \times 100$ , where DQ and Q are the dequenched and quenched donor fluorescence, respectively. Images were captured using a Nikon AIRSi.

**Statistical analysis.** Data are presented as the mean  $\pm$  S.D. Differences between the groups were assessed by an ANOVA followed by Tukey's *post-hoc* test. Comparisons between two groups were performed by Student's *t*-test.  $P < 0.05$  was considered significant.

### Conflict of Interest

The authors declare no conflict of interest.

**Acknowledgements.** This work was supported by grants from the National Natural Science Foundation of China (NO. 81100230, NO. 81070089,

NO. 81200071, and NO. 81270306), National Science and Technology Support Project (NO. 2011BAI15B02, NO. 2012BAI39B05 and NO. 2013YQ030923-05 and NO. 2014BAI02B01), the National Basic Research Program of China (NO. 2011CB503902), and the Key Project of the National Natural Science Foundation (No. 81330005).

- Zhai Y, Busuttill RW, Kupiec-Weglinski JW. Liver ischemia and reperfusion injury: new insights into mechanisms of innate-adaptive immune-mediated tissue inflammation. *Am J Transplant* 2011; **11**: 1563–1569.
- Fondevila C, Busuttill RW, Kupiec-Weglinski JW. Hepatic ischemia/reperfusion injury—a fresh look. *Exp Mol Pathol* 2003; **74**: 86–93.
- Jaeschke H. Reactive oxygen and ischemia/reperfusion injury of the liver. *Chem Biol Interact* 1991; **79**: 115–136.
- Kamo N, Ke B, Ghaffari AA, Shen XD, Busuttill RW, Cheng G et al. ASC/caspase-1/IL-1 $\beta$  signaling triggers inflammatory responses by promoting HMGB1 induction in liver ischemia/reperfusion injury. *Hepatology* 2013; **58**: 351–362.
- Ke B, Shen XD, Kamo N, Ji H, Yue S, Gao F et al. beta-catenin regulates innate and adaptive immunity in mouse liver ischemia-reperfusion injury. *Hepatology* 2013; **57**: 1203–1214.
- Kuboki S, Sakai N, Clarke C, Schuster R, Blanchard J, Edwards MJ et al. The peptidyl-prolyl isomerase, Pin1, facilitates NF-kappaB binding in hepatocytes and protects against hepatic ischemia/reperfusion injury. *J Hepatol* 2009; **51**: 296–306.
- Shin T, Kuboki S, Lentsch AB. Roles of nuclear factor-kappaB in postischemic liver. *Hepatology Res* 2008; **38**: 429–440.
- Uehara T, Xi Peng X, Bennett B, Satoh Y, Friedman G, Curran R et al. c-Jun N-terminal kinase mediates hepatic injury after rat liver transplantation. *Transplantation* 2004; **78**: 324–332.
- Inoue J, Ishida T, Tsukamoto N, Kobayashi N, Naito A, Azuma S et al. Tumor necrosis factor receptor-associated factor (TRAF) family: adapter proteins that mediate cytokine signaling. *Exp Cell Res* 2000; **254**: 14–24.
- Wajant H, Henkler F, Scheurich P. The TNF-receptor-associated factor family: scaffold molecules for cytokine receptors, kinases and their regulators. *Cell Signal* 2001; **13**: 389–400.
- Zapata JM, Krajewska M, Krajewski S, Kitada S, Welsh K, Monks A et al. TNFR-associated factor family protein expression in normal tissues and lymphoid malignancies. *J Immunol* 2000; **165**: 5084–5096.
- Schwenzer R, Siemienski K, Liptay S, Schubert G, Peters N, Scheurich P et al. The human tumor necrosis factor (TNF) receptor-associated factor 1 gene (TRAF1) is up-regulated by cytokines of the TNF ligand family and modulates TNF-induced activation of NF-kappaB and c-Jun N-terminal kinase. *J Biol Chem* 1999; **274**: 19368–19374.
- Zirlik A, Bavendiek U, Libby P, MacFarlane L, Gerdes N, Jagielska J et al. TRAF-1, -2, -3, -5, and -6 are induced in atherosclerotic plaques and differentially mediate proinflammatory functions of CD40L in endothelial cells. *Arterioscler Thromb Vasc Biol* 2007; **27**: 1101–1107.
- Rajandram R, Bennett NC, Wang Z, Perry-Keene J, Vesey DA, Johnson DW et al. Patient samples of renal cell carcinoma show reduced expression of TRAF1 compared with normal kidney and functional studies in vitro indicate TRAF1 promotes apoptosis: potential for targeted therapy. *Pathology* 2012; **44**: 453–459.
- McPherson AJ, Snell LM, Mak TW, Watts TH. Opposing roles for TRAF1 in the alternative versus classical NF-kappaB pathway in T cells. *J Biol Chem* 2012; **287**: 23010–23019.
- Oussa NA, Soumounou Y, Sabbagh L. TRAF1 phosphorylation on Serine 139 modulates NF-kappaB activity downstream of 4-1BB in T cells. *Biochem Biophys Res Commun* 2013; **432**: 129–134.
- Carpentier I, Beyaert R. TRAF1 is a TNF inducible regulator of NF-kappaB activation. *FEBS Lett* 1999; **460**: 246–250.
- Dunn IF, Sannikova TY, Geha RS, Tsitsikov EN. Identification and characterization of two CD40-inducible enhancers in the mouse TRAF1 gene locus. *Mol Immunol* 2000; **37**: 961–973.
- Tsitsikov EN, Laouini D, Dunn IF, Sannikova TY, Davidson L, Alt FW et al. TRAF1 is a negative regulator of TNF signaling. enhanced TNF signaling in TRAF1-deficient mice. *Immunity* 2001; **15**: 647–657.
- Jang HD, Chung YM, Baik JH, Choi YG, Park IS, Jung YK et al. Caspase-cleaved TRAF1 negatively regulates the antiapoptotic signals of TRAF2 during TNF-induced cell death. *Biochem Biophys Res Commun* 2001; **281**: 499–505.
- Lu YY, Li ZZ, Jiang DS, Wang L, Zhang Y, Chen K et al. TRAF1 is a critical regulator of cerebral ischaemia-reperfusion injury and neuronal death. *Nat Commun* 2013; **4**: 2852.
- Abu-Amara M, Yang SY, Tapuria N, Fuller B, Davidson B, Seifalian A. Liver ischemia/reperfusion injury: processes in inflammatory networks—a review. *Liver Transpl* 2010; **16**: 1016–1032.
- Georgiev P, Dahm F, Graf R, Clavien PA. Blocking the path to death: anti-apoptotic molecules in ischemia/reperfusion injury of the liver. *Curr Pharm Des* 2006; **12**: 2911–2921.
- He S, Atkinson C, Qiao F, Cianflone K, Chen X, Tomlinson S. A complement-dependent balance between hepatic ischemia/reperfusion injury and liver regeneration in mice. *J Clin Invest* 2009; **119**: 2304–2316.



25. Haeusgen W, Herdegen T, Waetzig V. The bottleneck of JNK signaling: molecular and functional characteristics of MKK4 and MKK7. *Eur J Cell Biol* 2012; **90**: 536–544.
26. Harding SJ, Browne GJ, Miller BW, Prigent SA, Dickens M. Activation of ASK1, downstream MAPKK and MAPK isoforms during cardiac ischaemia. *Biochim Biophys Acta* 2010; **1802**: 733–740.
27. Bluher M, Bashan N, Shai I, Harman-Boehm I, Tarnowski T, Avinaoch E et al. Activated Ask1-MKK4-p38MAPK/JNK stress signaling pathway in human omental fat tissue may link macrophage infiltration to whole-body Insulin sensitivity. *J Clin Endocrinol Metab* 2009; **94**: 2507–2515.
28. Malhi H, Gores GJ, Lemasters JJ. Apoptosis and necrosis in the liver: a tale of two deaths? *Hepatology* 2006; **43**(2 Suppl 1): S31–S44.
29. Montalvo-Jave EE, Escalante-Tattersfield T, Ortega-Salgado JA, Pina E, Geller DA. Factors in the pathophysiology of the liver ischemia-reperfusion injury. *J Surg Res* 2008; **147**: 153–159.
30. Colletti LM, Remick DG, Burtch GD, Kunkel SL, Strieter RM, Campbell DA Jr. Role of tumor necrosis factor-alpha in the pathophysiologic alterations after hepatic ischemia/reperfusion injury in the rat. *J Clin Invest* 1990; **85**: 1936–1943.
31. Volpes R, van den Oord JJ, De Vos R, Desmet VJ. Hepatic expression of type A and type B receptors for tumor necrosis factor. *J Hepatol* 1992; **14**: 361–369.
32. Jaeschke H, Lemasters JJ. Apoptosis versus oncotic necrosis in hepatic ischemia/reperfusion injury. *Gastroenterology* 2003; **125**: 1246–1257.
33. Pryhuber GS, Huyck HL, Roper JM, Cornejo J, O'Reilly MA, Pierce RH et al. Acute tumor necrosis factor-alpha-induced liver injury in the absence of tumor necrosis factor receptor-associated factor 1 gene expression. *Am J Pathol* 2005; **166**: 1637–1645.
34. Missiou A, Kostlin N, Varo N, Rudolf P, Aichele P, Ernst S et al. Tumor necrosis factor receptor-associated factor 1 (TRAF1) deficiency attenuates atherosclerosis in mice by impairing monocyte recruitment to the vessel wall. *Circulation* 2010; **121**: 2033–2044.
35. Wang CY, Mayo MW, Korneluk RG, Goeddel DV, Baldwin AS Jr. NF-kappaB antiapoptosis: induction of TRAF1 and TRAF2 and c-IAP1 and c-IAP2 to suppress caspase-8 activation. *Science* 1998; **281**: 1680–1683.
36. Speiser DE, Lee SY, Wong B, Arron J, Santana A, Kong YY et al. A regulatory role for TRAF1 in antigen-induced apoptosis of T cells. *J Exp Med* 1997; **185**: 1777–1783.
37. Hattori K, Naguro I, Runchel C, Ichijo H. The roles of ASK family proteins in stress responses and diseases. *Cell Commun Signal* 2009; **7**: 9.
38. Noguchi T, Takeda K, Matsuzawa A, Saegusa K, Nakano H, Gohda J et al. Recruitment of tumor necrosis factor receptor-associated factor family proteins to apoptosis signal-regulating kinase 1 signalosome is essential for oxidative stress-induced cell death. *J Biol Chem* 2005; **280**: 37033–37040.
39. Sughra K, Birbach A, de Martin R, Schmid JA. Interaction of the TNFR-receptor associated factor TRAF1 with I-kappa B kinase-2 and TRAF2 indicates a regulatory function for NF-kappa B signaling. *PLoS One* 2010; **5**: e12683.
40. Zhang Q, Zhang G. Activation and autophosphorylation of apoptosis signal-regulating kinase 1 (ASK1) following cerebral ischemia in rat hippocampus. *Neurosci Lett* 2002; **329**: 232–236.
41. Uehara T, Bennett B, Sakata ST, Satoh Y, Bilter GK, Westwick JK et al. JNK mediates hepatic ischemia reperfusion injury. *J Hepatol* 2005; **42**: 850–859.
42. Lutz J, Thurmel K, Heemann U. Anti-inflammatory treatment strategies for ischemia/reperfusion injury in transplantation. *J Inflamm (Lond)* 7: 27.
43. Sakai N, Van Sweringen HL, Quillin RC, Schuster R, Blanchard J, Burns JM et al. Interleukin-33 is hepatoprotective during liver ischemia/reperfusion in mice. *Hepatology* 2012; **56**: 1468–1478.
44. Wang XA, Zhang R, Jiang D, Deng W, Zhang S, Deng S et al. Interferon regulatory factor 9 protects against hepatic insulin resistance and steatosis in male mice. *Hepatology* 2013; **58**: 603–616.
45. Wang XA, Zhang R, She ZG, Zhang XF, Jiang DS, Wang T et al. Interferon regulatory factor 3 constrains IKKbeta/NF-kappaB signaling to alleviate hepatic steatosis and insulin resistance. *Hepatology* 2013; **59**: 870–885.
46. Ocuin LM, Zeng S, Cavnar MJ, Sorenson EC, Bamboat ZM, Greer JB et al. Nilotinib protects the murine liver from ischemia/reperfusion injury. *J Hepatol* 2012; **57**: 766–773.
47. Jiang DS, Bian ZY, Zhang Y, Zhang SM, Liu Y, Zhang R et al. Role of interferon regulatory factor 4 in the regulation of pathological cardiac hypertrophy. *Hypertension* 2013; **61**: 1193–1202.
48. Jiang DS, Luo YX, Zhang R, Zhang XD, Chen HZ, Zhang Y et al. Interferon regulatory Factor 9 protects against cardiac hypertrophy by targeting myocardin. *Hypertension* 2013; **63**: 119–127.



**Cell Death and Disease** is an open-access journal published by Nature Publishing Group. This work is licensed under a Creative Commons Attribution-NonCommercial-ShareAlike 3.0 Unported License. The images or other third party material in this article are included in the article's Creative Commons license, unless indicated otherwise in the credit line; if the material is not included under the Creative Commons license, users will need to obtain permission from the license holder to reproduce the material. To view a copy of this license, visit <http://creativecommons.org/licenses/by-nc-sa/3.0/>

Supplementary Information accompanies this paper on Cell Death and Disease website (<http://www.nature.com/cddis>)